SIMULATION OF FIXED-BED

ION EXCHANGE PROCESSES

By

KEITH JOSEF WILSON

Bachelor of Science

Tennessee Technological University
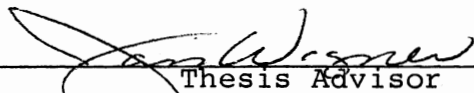
Cookeville, Tennessee

1982

Submitted to the faculty of the
Graduate College of the
Oklahoma State University
in partial fulfillment
of the requirements for
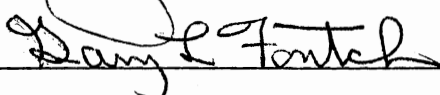the degree of
MASTER OF SCIENCE
December, 1983

SIMULATION OF FIXED-BED

ION EXCHANGE PROCESSES

Thesis Approved:

_____
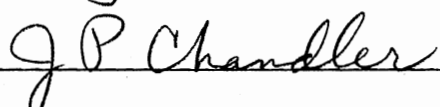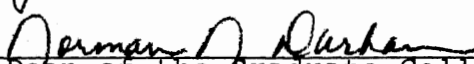Thesis Advisor

_____

_____

_____
Dean of the Graduate College

ii

PREFACE

A numerical model for predicting breakthrough curves of general fixed-bed ion exchange processes was developed. In the model, the column operated under local equilibrium, and hydrodynamic dispersion was included as a transport mechanism. A numerical dispersion coefficient was introduced to account for truncation error in the numerical approximation. The model is capable of predicting breakthrough data for systems whose equilibria are described by linear, Langmuir, or Freundlich isotherms.

An interactive computer program was developed to implement the numerical solution algorithm. Test calculations were performed to check the validity of the numerical approximation technique, and to compare predicted data with experimental data from the literature.

TABLE OF CONTENTS

LIST OF TABLES

LIST OF FIGURES

Figure   Page

ix

NOMENCLATURE

A	column cross sectional area
C	solution-phase concentration
C_{in}	inlet solution concentration
$C_{initial}$	initial resin-phase concentration
C_o	concentration at $z = 0$
C_s	resin-phase concentration
C_{smax}	maximum resin-phase concentration
C_T	total concentration in resin and solution phases
D_c	column diameter
D_z	overall dispersion coefficient
D_{zhydro}	physical dispersion coefficient
D_{znum}	numerical dispersion coefficient
D_{ztot}	total dispersion in numerical approximation
D_p	resin particle diameter
$F, f(c)$	equilibrium isotherm parameter
g_c	gravitational constant
i	spatial grid node
j	temporal grid node
K, F_k	equilibrium constant
L	bed length
M_L	mass of ion in solution phase
M_s	mass of ion in resin phase

n, F_n equilibrium exponent

Q_L dispersive ionic flux

Re_p particle Reynolds number, $D_p V_z \rho_f / \mu_f$

r_0 resin particle radius

t time

$\dot{V}$ solution volumetric flow rate

V_0 superficial velocity

V_T total bed volume

V_z average interstitial velocity

z spatial coordinate

Greek Symbols

ε resin porosity

μ_f fluid viscosity

ρ_f fluid density

Θ order of error in Taylor series expansions

CHAPTER I

INTRODUCTION

The purpose of the herein described research was to develop a numerical model to simulate the performance of fixed-bed ion exchange columns for general ion exchange systems. The systems of interest were those which involved gel-type ion exchange resins and two exchanging ions which exhibited linear, Langmuir, or Freundlich equilibrium relationships.

The objective was to develop a model which would require a minimum of experimental data for evaluation. Since solution-resin equilibrium is one of the first properties to be evaluated for a proposed ion exchange system, the model was developed on the basis of equilibrium theory which neglects all mass transfer inefficiencies in the solution and resin phases, describes the rate of exchange as infinite, and describes the solution to be in equilibrium with the resin at all times and at all points in the fixed bed. The rate term in the material balance equation was replaced by a function of the equilibrium relationship.

Industrial applications of ion exchange include the purification of water sources, separation of rare earth metals, and decontamination of nuclear reactor cooling water. A common process arrangement consists of vertical fixed-bed columns which are used to contact the solution and

the ion exchange material. The effect of changes in operating conditions on the performance of ion exchange processes is needed to determine the optimum process configuration, operating conditions, and column design. Most process development requires scale-up due to the complexity of ion exchange processes. Considerable effort would be saved if optimum operating conditions could be determined, through the use of a rating program on a pilot-scale operation, and then included in the scaled-up process. Therefore, a reliable mathematical model, which requires a minimum of experimental data, could be used by engineers to avoid extensive experimentation with actual columns in the determination of optimum process operating conditions.

As discussed in Chapter 2, determination of the parameters necessary for a kinetic treatment of ion exchange requires extensive experimentation. Equilibrium theory, which requires only column characteristics and equilibrium data for evaluation, has been successfully used in the isolation of potential ion exchange systems.

The convection-dispersion (C-D) equation, which governs the transient behavior of an ion exchange column with both convective and dispersive material transport accounted for, was derived. The solution of the C-D equation, which has historically been difficult to approximate numerically, was then approximated by an implicit finite-difference technique. A numerical dispersion correction term was included to account for truncation error inherent in the approximation of the partial derivatives.

The approximation was developed from a two-point temporal, three-point spatial finite-difference grid network, which insured consistent orders of truncation error in both time and space. The numerical

approximation was validated by comparison with closed-form analytical solutions for the linear form of the C-D equation.

The model was evaluated by comparing predicted column performance with the corresponding experimental data for both linear and nonlinear systems. Parameters of the model were adjusted to give agreement in the breakthrough times for all systems studied and the entire breakthrough curve for the linear-equilibrium system. Sensitivity tests on four system parameters were conducted to aid in further model development.

CHAPTER II

LITERATURE REVIEW

This chapter gives a review of past work in three areas which the
present work combines. The characteristics of ion exchange are briefly
discussed with an aim to justify the assumption of local equilibrium,
between solution and resin, used in the present model. Applications of
equilibrium theory are then discussed. The final section concerns the
numerical solution of the convection-dispersion equation which is the
foundation of the present study.

Characteristics of Ion Exchange

Solid ion-exchange materials consist of a matrix, held together
(cross-linked) by chemical and physical bonding, and of chemically
functional groups which are bonded to the matrix. The matrix is
absorbent to suitable solvents. When this sorption occurs, the
functional groups dissociate to form two types of ions. The first type,
of either positive or negative charge, is immobile and remains bonded to
the matrix. The second type of ion is oppositely charged to the first
type. This ion is mobile and free to move through the solvent-matrix
system and into the external solution.

Most solid ion-exchange materials, the majority of which are
addition copolymers prepared from vinyl monomers, consist of a
hydrocarbon matrix to which the functional groups are bonded. An

4

example of this type of resin is cross-linked polystyrene which has functional groups introduced after polymerization, by treating the polymer with sulfuric acid to produce sulfonic groups.

Ion exchange occurs when the mobile ions, originally in the solvent-matrix system, move into the external solution and different ions of similar charge move from the external solution into the solvent-matrix system. The exchanging ions are termed counter ions, while the ions originally in the external solution, of opposite charge to the counter ions, are called co-ions. The ion exchange is termed cation exchange if the counter ions are positively charged, and anion exchange if the counter ions are negatively charged.

For the condition of electroneutrality to be met, the exchange of counter ions must be stoichiometric. Also, exchange of counter ions is usually reversible in that conditions can be found under which the same counter ion is exchanged into and out of the solvent-matrix system. The solvent-matrix system will preferably sorb certain counter ions. This property, termed selectivity, has given ion exchange its potential as a separation technique in industrial and laboratory applications.

Since the exchange reaction occurs extremely rapidly, the rate of exchange is controlled by diffusion of ions in the resin pores and through the external solution. Either of these diffusional mechanisms, or some combination of both, may be rate limiting.

A rigorous quantitative theory for the general kinetics of fixed-bed ion-exchange processes is not feasible owing to the complexity of both ion exchange and the hydrodynamics of porous media. Even the much simpler problem of batch ion exchange kinetics has been solved only for certain limiting cases (Helfferich, 1962). For this reason, the

assumption of local equilibrium, where mass-transfer inefficiencies are neglected, is appealing for the general model under consideration.

Two basic varieties of equilibrium are found in column exchange operations. Favorable exchange equilibrium occurs when the counter ion in the feed is preferred by the ion exchanger. Any spread in the exchange front is counteracted by delay of preferred ions ahead of the front and displacement of nonpreferred ions behind the front. A sharp boundary between converted solution and unconverted solution results. The sharpness of the boundary is proportional to the strength of preference.

In unfavorable exchange equilibrium, the ion initially present in the resin is preferred by the resin. Feed ions which are ahead of the exchange boundary are held less strongly than the favored ions, while resin ions behind the boundary are delayed. The boundary becomes increasingly diffuse through the length of the column.

At breakthrough, when the effluent concentration rises above some critical level, the bottom layers of resin are not completely converted. Therefore, the breakthrough capacity is less than the total column capacity. A measure of column efficiency is given by the degree of column utilization, which is defined as the ratio of the breakthrough to the overall capacities and is high when the exchange front is sharp. In addition, a system which exhibits a sharp boundary allows for a greater flow rate and a smaller column due to higher exchange efficiency.

On the macroscopic level, some equilibrium theories involve the concept of "effective plates," the solution in a vertical section of the column attaining equilibrium before moving to the next section

(Helfferich, 1962). Deviations from local equilibrium are accounted for by assigning each section a finite height, called the effective plate height, which must be determined experimentally. These theories then assume mixing in the plates to cause boundary spreading. Other equilibrium theories, such as that of DeVault (1943), assume that equilibrium is attained by each resin particle. These theories are especially useful for unfavorable equilibrium since the boundary rapidly diffuses and approaches the pattern in which local equilibrium prevails. The process then becomes independent of the location in the column. These theories are well suited to multicomponent systems and systems whose isotherms are partly favorable and partly unfavorable.

On the microscopic level, ion exchange rates are controlled by film and particle diffusion. Equilibrium theories neglect these mechanisms, as the exchange rate is infinite. Film diffusion control can usually be eliminated in fixed beds of spherical resin beads by using small beads and low flow rates. For spherical ion-exchange beads, Gilliland (1953) gives an empirical relation for the Nernst film thickness as a function of r_0, the bead radius. r_0 dereases with decreasing particle size, so that film thickness and the importance of film diffusion decrease in the same manner. Helfferich (1962) reported typical film thicknesses on the order of 10^{-2} to 10^{-3} cm.

Particle diffusion control is somewhat more complex because it involves such parameters as the degree of cross-linking in the resin, ionic diffusivities, and intraparticle electrical effects. The evaluation of resin-side parameters requires extensive experimental work.

High rates of exchange are favored by a low degree of cross-linking, which is accompanied by increased swelling of the resin. In this condition, the resin matrix interferes with ionic diffusion to a lesser extent than with higher cross-linking in an unswollen resin, and the diffusing ions are able to move through the resin more rapidly. Ionic fluxes are coupled by the imposed condition of electroneutrality. The electric field generated by the diffusion of the ions produces an electric transference of counter ions in the direction of the slower diffusing ion. This electric transference is superimposed on the diffision. The resulting net fluxes, but not necessarily velocities, of the counter ions are equal, while the purely diffusional fluxes, as a rule, are not. The Nernst-Plank equation, which expresses the net flux as the sum of diffusional and electrical fluxes, must be solved for each species present (Helfferich, 1962). In light of the necessity of electroneutrality and the strength of the electric potential which develops under even slight deviations from neutrality, the electrical transference could overshadow the purely diffusional transference.

Another factor which influences particle diffusion of ions is convection conductivity. When diffusion begins, there are more counter ions, than co-ions, in the particle. Momentum is transferred to the solvent molecules by the diffusing counter ions, and convection occurs in the direction of counter-ion transfer. The convection of pore liquid is superimposed on the migration of the ions relative to the pore liquid. The ions move faster, relative to the matrix, than they would during ordinary diffusion. In usual resins, the pore width is smaller than the Debye-Huckel ionic cloud, so that convection occurs through the

entire pore cross section rather than at the walls only (Bjerrum and Manegold, 1928).

Complete description of the electrical effects in the exchanger can be given in terms of irreversible thermodynamics, but the treatment is rather abstract. Therefore, a model is proposed (Helfferich, 1962).

The ion exchanger is considered as a porous system which is homogeneous on a macroscopic scale. Transference relative to the matrix results from superposition of transference relative to the pore liquid and transport by convection of the pore liquid. Some fundamental limitations exist even for this simple model. The Nernst-Einstein relation for ionic mobility disregards coupling of fluxes other than by induced convection. The model also implies that pore liquid ions travel at the same rate through the pore cross section, disregarding ionic interactions with the matrix (Spiegler and Coryell, 1953). Individual ionic-interaction parameters would be required for improvement of the model, but the mathematics would be greatly complicated.

The parameters needed for evaluation of the model include the intraparticle electric potential gradient, ionic diffusivities, specific flow resistance, and specific conductivity of the resin. These parameters are determined, for a particular system, through extensive experimentation. This approach is in appropriate for general considerations.

The assumption of local equilibrium, due to its simplicity, is the most useful way of treating the kinetics of fixed-bed ion-exchange processes for general systems. Rigorous mathematical treatment of the equilibrium theory in fixed beds can be found in the literature; see,

for example, Goldstein (1953). However, the solutions presented are valid for linear isotherms only.

In summary, equilibrium theory, which requires only column characteristics and equilibrium data for evaluation, is based on the following assumptions:

1. Equilibrium between solution and exchange resin exists at all times, and at all points within the exchanger bed;

2. The bed is homogeneous. A random distribution of void spaces exists within the resin;

3. Flow is in the axial direction only;

4. Secondary processes, such as neutralization, precipitation, and complex formation are neglected. Furthermore, in the absence of chemical reactions, ion exchange usually evolves or consumes little heat. Enthalpy changes during exchange are usually less than 2 kcal/mole (Helfferich, 1962). Therefore, the ion-exchange column is assumed to operate isothermally. Additionally, for the dilute solutions of primary interest, any changes in solution density or viscosity, during the exchange process, are small. So, for isothermal operation with dilute solutions, the density and viscosity of the solution are constant.

Equilibrium Theory of Ion Exchange

The performance of an ion exchange operation is governed by exchange stoichiometry, solution-exchanger equilibrium, and exchange rate, as well as the process arrangement used. Equilibrium theory involves consideration of stoichiometry and equilibrium only.

Although calculations based on equilibrium theory may yield concentrations in the bed, or effluent histories, quite different from those obtained physically, these calculations represent the optimum performance of the exchange operation. The calculations may be extremely useful in the prediction of the behavior of new systems and in the interpretation of experimental results.

Equilibrium theory calculations can be useful in the exclusion of a proposed process on the basis of equilibrium data alone. The determination of additional process parameters is not necessary. The effect of changes in process variables, such as solution flow rate, column size, and operating temperature, can also be predicted. Equilibrium theory accurately predicts any periods of constant-effluent concentration which may occur, which is especially important for multicomponent exchange. Under certain operating conditions, namely low flow rate, unfavorable equilibrium, and high diffusivities in the exchanger phase, equilibrium theory calculations may provide a good approximation to actual column performance.

The first equilibrium theories pertained to chromatography. Wilson (1940) qualitatively described chromatographic analysis by neglecting intraparticle diffusion and establishing instantaneous equilibrium between the solution and the sorbent. The width of the adsorption band was also assumed to remain constant during the chromatographic development. Observed widening of the adsorption band was attributed to lack of equilibrium between sorbent and solution phases.

DeVault (1943) treated single component sorption rigorously, and discussed multicomponent sorption qualitatively, in terms of equilibrium operation and a general isotherm. Wilson (1940) had shown that solid-

phase concentration was a discontinuous function of distance along the bed, while DeVault's study indicated that this was true if the solute was strongly adsorbed. Weiss (1943) extended DeVault's work to linear, Langmuir, and Freundlich isotherms, with results similar to those of DeVault.

Walter (1945) used the equilibrium theory and developed equations for two-component adsorption. As with DeVault (1943) and Weiss (1943), the diffuse nature of the exchange-front boundaries was investigated.

A chromatographic column, if operated at equilibrium conditions, could be used to determine the equilibrium isotherm of a system of interest. An obvious advantage of this method is that a single experiment gives an almost unlimited number of points of the isotherm. Glueckauf (1947) has investigated this experimental use of equilibrium theory.

The analogy between the mode of operation of a distillation column and that of an ion-exchange column allowed modification of local equilibrium theory. The ion-exchange column was treated as a series of "plates." As solution flowed through each plate, equilibrium between the solution and the exchanger occurred. The plate was of sufficient length, referred to as the "height equivalent of one theoretical plate (HETP)," to accomplish this equilibration.

Martin and Synge (1941) found that, under the limited conditions of constant equilibrium coefficient, the width of the adsorption band predicted by their HETP theory was similar to the experimentally observed band width. By using solution volume and resin mass, rather than theoretical plate area and height, respectively, Mayer and Tompkins (1947) simplified the theory of Martin and Synge (1941). The approach

of Mayer and Tompkins (1947) was directly applicable to determining eluate composition, as well as to predicting the distribution of the various substances in the column. Application of their method to rare-earth separations at near-equilibrium conditions showed good agreement with experimental data.

Glueckauf (1955) reported that the theoretical-plate approach was important in improving the efficiency of ion-exchange operations. He found that the column efficiency was improved by making the HETP sufficiently small and the total number of plates sufficiently large.

Pandya et al. (1965) applied stagewise calculations to the equilibrium-performance evaluation of ion-exchange columns for the prevention of scale formation during sea water evaporation. The work of Martin and Synge (1941) and Mayer and Tompkins (1947) was extended to yield approximate results for multicomponent systems with nonlinear equilibrium isotherms.

Local-equilibrium theory was applied to process design calculations by Frisch and McGarvey (1959). Axial dispersion was neglected, and the work of Walter (1945) was extended to predict the effects of regeneration level and regenerant purity on maximum regenerated capacity, equilibrium leakage during the exhaustion cycle, and elute composition. Good estimation of column performance was accomplished even with extrapolated data.

The University of California's Sea Water Conversion Laboratory used the equilibrium model extensively in the design of a sea-water-softening process, in the analysis of different schemes for saline-water pretreatment or desalination, and for studying the dynamics of multicomponent ion-exchange systems. Of particular importance in a

desalination process was the removal of constituents, from the brine, which deposited as boiler scale in an evaporator.

Klein et al. (1963) used the equilibrium model to select suitable ion-exchange resins for the sea-water-treatment process. Optimum values of the product of selectivity coefficient and resin exchange capacity were used to eliminate undesirable exchange materials. Within the useful group of resins, marked trends with cross-linking, total and individual ionic concentrations, and temperature were not apparent. Klein et al. (1965) used the equilibrium model to develop rules for outlining the overall concentration profiles for multicomponent systems. The rules were used to determine the number of constant-composition zones, the signs of the slopes of the concentration profiles, and the order of points at which the component concentrations could become zero. The concentration profiles could then be converted to effluent concentration histories. Klein et al. (1968) performed a design and cost analysis of the process which was recommended by the equilibrium studies.

Klein and Vermeulen (1974) summarized the theoretical aspects of the equilibrium operation of pure ion exchange that had been used in the previous studies. Column dynamics and ion exchange accompanied by chemical reaction, as well as design applications in cyclic operation, were considered.

Solution of the Convection-Dispersion Equation. The parabolic partial differential equation which describes one-dimensional flow in porous media is

$$F \frac{\partial C}{\partial t} = D_z \frac{\partial^2 C}{\partial z^2} - V_z \frac{\partial C}{\partial z} \qquad (1)$$

where

C = solution phase concentration, lb/ft^3,

F = isotherm proportionality function, $F(C,\varepsilon)$,

D_z = dispersion coefficient, ft^2/sec,

and

V_z = average intersitital velocity, ft/sec.

The solution to this parabolic equation has been historically difficult to approximate numerically.

Standard implicit finite-difference techniques, such as the method of Crank and Nicolson (1947), developed oscillations and frontal smearing due to truncation of a Taylor series in the numerical approximation. Von Neumann and Richtmeyer (1950) attributed these difficulties to shock fronts which manifested themselves mathematically as discontinuities in system properties. The shocks occurred when the value of D_z was zero or much smaller than the value of V_z. Equation 1 became more hyperbolic, than parabolic, under these circumstances. These authors proposed that the difficulties could be decreased by using an artificially large value of D_z, which restored some of the parabolic character of Equation 1. The effect on the numerical solution was to give the shock fronts a thickness on the order of the numerical-grid spacing and smear out the discontinuities so that the dependent variable varied rapidly, but continuously.

Peaceman and Rachford (1962) developed a difference analogue to Equation 1 by replacing the spatial derivatives with difference quotients evaluated at t_j and t_{j+1}. The resulting equation was referred to as a "time-centered" difference equation and was given as

$$\frac{D_z}{(\Delta z)^2} (C_{i-1}^j - 2C_i^j + C_{i-1}^j - 2C_{i+1}^{j+1} + C_{i+1}^{j+1}) \tag{2}$$

$$+ \frac{V_z}{\Delta z} (\overline{C}_{i-1/2}^j + \overline{C}_{i-1/2}^{j+1} - \overline{C}_{i+1/2}^j - \overline{C}_{i+1/2}^{j+1}) = \frac{2F}{\Delta t} (C_i^{j+1} - C_i^j)$$

where $\overline{C}$ was a representation of concentration at the spatial node, $i+1/2$.

Two choices of $\overline{C}$ were considered:

1. Distance-Centered

$$\overline{C}_{i+1/2} = (C_{i+1} + C_i)/2; \tag{3}$$

2. Backward-in-Distance

$$\overline{C}_{i+1/2} = C_i. \tag{4}$$

Substitution of Equation 4 into Equation 2 gave "off-centering" in the direction opposite to flow. Calculations with Equation 2 showed overshoot for the distance-centered difference equation, and frontal smearing for the backward-in-distance difference equation.

To avoid these characteristics, any overshoot was added ahead of the front to C_{i+1}^{j+1}, and C_i^{j+1} was decreased by the same amount of overshoot. Results were improved with this "transfer of overshoot" method. However, application of this method to the two-dimensional problem with zero dispersion indicated that the method contained a numerical dispersion of the same order of magnitude as the hydrodynamic dispersion.

Stone and Brian (1963) developed a rigorous method to determine the accuracy of various finite-difference approximations of the linear form of Equation 1. Their analysis was based on the adjustment of arbitrary weighting parameters to obtain a finite-difference approximation which

traveled the low-frequency harmonics of the analytical solution to the C-D equation at velocities close to the convection velocity, V_z. Cyclic use of weighting parameter values was also observed to enhance the convection properties of the finite-difference approximations to the C-D equation. This treatment succeeded in reducing the oscillation and numerical dispersion, but some oscillatory behavior was still present in steep-front regions.

Garder, Peaceman, and Pozzi (1964) proposed a method of numerical solution of the C-D equation based on characteristic paths. The method involved moving points, applied to multiple dimensions, accounted for any amount of hydrodynamic dispersion, and introduced no numerical dispersion. The equations of the characteristic paths for the one-dimensional problem were

$$\frac{dz}{dt} = \frac{V_z}{\varepsilon} \tag{5}$$

and

$$\frac{dC}{dt} = \frac{D_z}{\varepsilon} \frac{\partial^2 C}{\partial z^2} \tag{6}$$

A stationary finite-difference grid was defined, and a random set of moving points was introduced into the grid intervals. New positions of the points were calculated from Equation 5. The concentration change due to dispersion was calculated from Equation 6, and each moving point was assigned an updated concentration. This procedure was repeated for each time step. The dispersive contribution was calculated explicitly, which imposed a stability limitation on the time increment size.

Price et al. (1968) presented numerical approximations of the C-D equation based on variational methods. Galerkin's method, with Chapeau basis functions, was used to obtain difference approximations of the form

$$\frac{2}{3}\frac{dC(\Theta)}{d\Theta} + \frac{1}{6}\left(\frac{dC_i(\Theta)}{d\Theta} + \frac{dC_{i-1}(\Theta)}{d\Theta}\right)$$

$$= \frac{2C_i(\Theta)}{h^2} + \frac{(1 - \frac{\lambda h}{2})}{h^2} C_{i+1}(\Theta) + \frac{(1 + \frac{\lambda h}{2})}{h^2} C_{i=1}(\Theta)$$

(7)

where

$$\lambda = \frac{V_z L}{D_z},$$

$$\Theta = \frac{D_z t}{\varepsilon L^2},$$

h = mesh spacing,

and

L = system length.

Calculations based on this method were compared to calculations based on the methods of Price et al. (1966), and Garder et al. (1964). Increased accuracy and decreased computer time were observed. A variable interpolation method, which used two types of basis functions depending upon the proximity to the front, was also presented.

Laumbach (1975) canceled some of the error in the approximation of the convection term with that of the accumulation term. Spatial truncation error was introduced in the approximation of the accumulation term, $\partial C/\partial t$, and an arbitrary parameter, w, was used to give the approximation of the C-D equation as

$$(1 - w) \left(\frac{c_i^{j+1} - c_i^j}{\Delta t}\right) + \frac{w}{2} \left(\frac{c_{i+1}^{j+1} - c_{i+1}^j + c_{i-1}^{j+1} - c_{i-1}^j}{\Delta t}\right) \qquad (8)$$

$$= \frac{D_z}{2(\Delta z)^2} \left(c_{i+1}^{j+1} - 2c_i^{j+1} + c_{i+1}^{j+1} + c_{i+1}^j - 2c_i^j + c_{i+1}^j\right)$$

$$- \frac{V_z}{4\Delta z} \left(c_{i+1}^{j+1} - c_{i-1}^{j+1} + c_{i+1}^j - c_{i-1}^j\right),$$

where

$$w = \frac{1}{3} + \frac{r^2}{6},$$

and

$$r = \frac{\Delta t}{\Delta z}.$$

As $\Delta t \rightarrow 0$, Equation 8 reduced to a form identical to that of Stone and Brian (1963) and Price et al. (1968). This discretization was of the semi-implicit type and resulted in a set of linear equations which could be solved by Gaussian elimination.

Larson (1982) presented a method which reduced numerical dispersion by updating the component fluxes from adjacent finite-difference grid blocks. The treatment was analogous to the method of characteristics in that the equations explicitly expressed the velocities at which fixed values of concentration were propagated through the system.

Fanchi (1983) has presented a truncation error analysis which outlined equations for a numerical dispersion coefficient, the form of which depended upon the difference techniques used in the numerical approximation. Total dispersion consisted of a physical contribution and a numerical contribution. Numerical dispersion was reduced by subtracting the numerical dispersion coefficient from the hydrodynamic

dispersion coefficient which appeared in the numerical model. Improvement in the accuracy of the numerical solution was observed.

The above studies used exact solutions, where possible, for comparative purposes. Analytical solutions to the one-dimensional C-D equation have been reported by Brenner (1962) and Hunt (1978). Brenner (1962) considered beds of finite length, while Hunt (1978) gave solutions for semi-finite beds for both instantaneous and continuous sources. The solution of interest is

$$C(z,t) = \frac{\dot{M} \exp(\frac{zV_z}{2D_z})}{2 \, \varepsilon \, V_z} \left[\exp\left(- \frac{|z|V_z}{2D_z}\right) \operatorname{erfc}\left(\frac{|z| - V_z t}{2 \sqrt{D_z t}}\right) \right.$$

$$\left. - \exp\left(\frac{|z| V_z}{2D_z}\right) \operatorname{erfc}\left(\frac{|z| + V_z t}{2 \sqrt{D_z t}}\right) \right], \tag{9}$$

where $\dot{M}$ = solution flow rate, ft^3/sec. Equation 9 will be used for comparative purposes in the present work.

CHAPTER III

PROPOSED MODEL FOR FIXED-BED ION EXCHANGE

This chapter has two primary functions. The first is to define the ion-exchange system being modeled, with an emphasis on basic assumptions. The second is to develop the mathematical model for the defined system.

Definition of the Ion-Exchange System Being Modeled

The specific system being defined is shown in Figure 1 and is described by the following. A solution having constant volumetric flow rate, $\dot{V}$, and constant inlet concentration, C_{in}, is fed downward to a fixed-bed, cylindrical, vertical column having inside dimeter, D_c, and inside cross-sectional area, A. The solution contains a single ionic species of interest and may also contain small amounts of nonelectrolyte components. The concentration of the solution leaving the bottom of the column is C_{out}. Bulk average flow is in the z-direction only, with constant interstitial velocity, V_z. Concentrations of the solid and solution phases are indepedent of the r-direction. The column is packed to a height, L, with a spherical ion-exchange resin. Resin shrinkage and expansion is neglected. The resin bed is homogeneous, with a constant porosity, ε, throughout. The initial concentration in the bed, $C_{initial}$, applies to all parcels of solution in the bed. The rate of ion exchange is infinite, i.e. mass transfer resistances in the resin

INLET SOLUTION:
$\dot{V}$, ft^3/sec
C_{in}, lbm/ft^3
Constant transport properties
P_{in}, psi

Ion Exchange Resin

ΔZ

$C_i(t)$

$C_i(o) = C_{initial}$

D_c

Column Operates Isothermally

r

$Z=0$

Z

Z_i

Z_{i+1}

$Z=L$

OUTLET SOLUTION:
$\dot{V}$, ft^3/sec
C_{out}, lbm/ft^3
P_{out}, psi
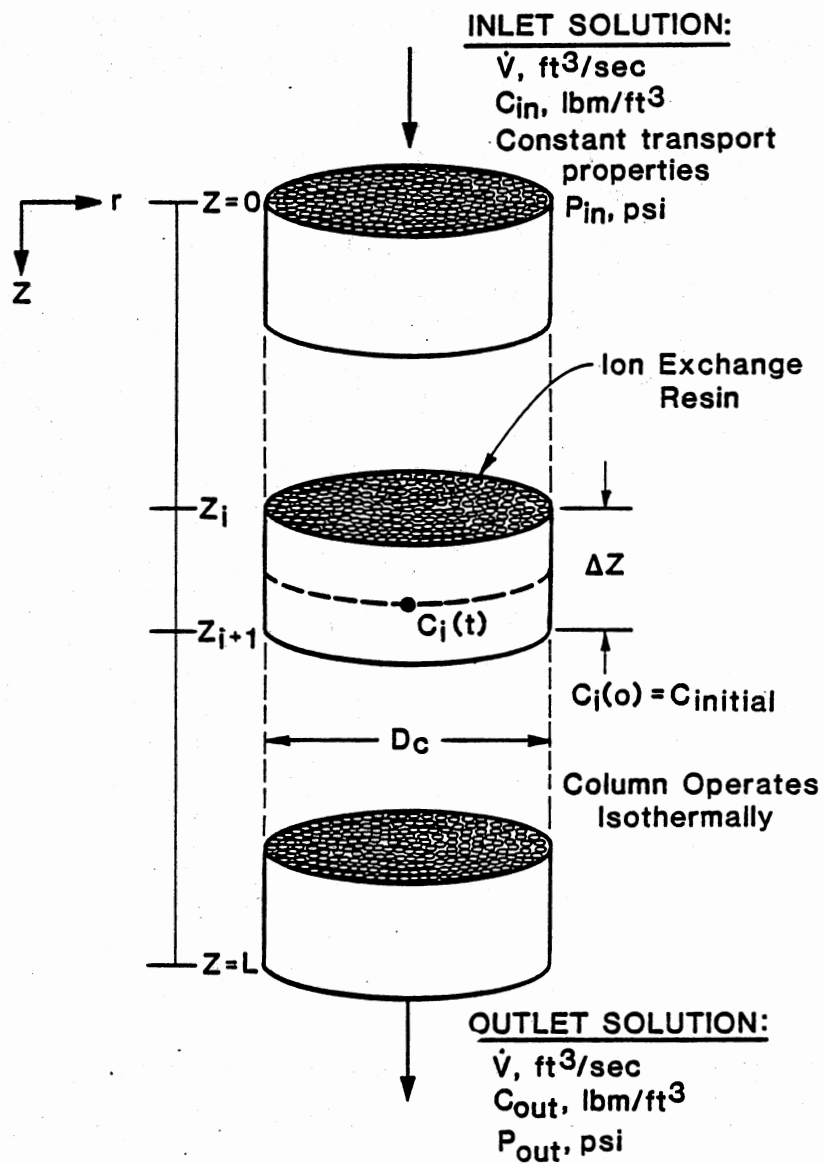
Figure 1. Schematic Diagram of Ion Exchange Column

particles, and in the solution layer surrounding the resin particles, are neglected. This implies that the solution and resin are in equilibrium at all times. The column operates approximately iso-thermally and at relatively low ionic concentrations. Therefore, the solution density and viscosity remain essentially constant throughout the column. As solution flows through the bed the exchange front is spread in the z-direction. This phenomena is described by a Fickian diffusion model and dispersive flux is given by $Q = D_z \frac{\partial C}{\partial z}$, where D_z is a constant dispersion coefficient. However, dispersion in the r-direction is neglected. Also, bulk convection overshadows transport by ionic diffusion, and the latter mechanism is neglected.

Basic Elements of the Model

The four basic elements of the proposed model are listed below. (1) The column is divided axially into a number of cylindrical volume elements. The concentrations of the solution and resin phases are constant across the diameter of an infinitesimally thin slice of an element. (2) A general mass balance is derived, based on applicable transport mechanisms, and applies to all volume elements. (3) The terms of the mass balance equation are approximated for numerical evaluation. Any empirical parameters are defined from available literature, or are obtainable experimentally. (4) The set of simultaneous equations, which arises from application of the approximated material balance to all spatial increments of the column, is put into a form for numerical solution with time.

Development of the Model

Consider the volume element, of thickness Δz, shown in Figure 1. A mass balance equation of the form

$$\text{mass in} - \text{mass out} = \text{mass accumulated} + \text{mass produced} \tag{10}$$

can be written for the element over any time increment, Δt . Mass enters and exits the element by convective and dispersive fluxes. Mass is accumulated by ionic transfer during the ion-exchange process. No mass is created or destroyed, so the production term is eliminated.

Defining these quantities in terms of system parameters and substituting into Equation 10 gives

$$\Delta t \ V_z \ AC|_z - \Delta t \ V_z AC|_{z+\Delta z} \ \cdot \ \cdot \ \cdot \ \text{Convection} \tag{11}$$

$$+ \ \Delta t \ AQ_L|_z - \Delta t \ AQ_L|_{z+\Delta z} \ \cdot \ \cdot \ \cdot \ \text{Dispersion}$$

$$= \Delta z \ A(C_S + C)|_t - \Delta z A(C_S + C)|_{t+\Delta t} \ \cdot \ \cdot \ \cdot \ \text{Accumulation,}$$

where

$Q_L \ = \ D_z \dfrac{\partial C}{\partial z}$,

$C \ = \ $ liquid phase concentration, lb ion/ft^3 solution,

$C_S \ = \ $ solid phase concentration, lb ion/ft^3 solid,

and

$|_z \ = \ $ "evaulated at z."

Rearranging Equation 11, dividing by $A\Delta t\Delta z$, and taking the limit as Δz and Δt approach zero gives

$$\lim_{\Delta z \to 0} \left(\frac{V_z C|_{z+\Delta z} - V_z C|_z}{\Delta z} + \frac{Q_L|_{z+\Delta z} - Q_L|_z}{\Delta z} \right) \tag{12}$$

$$= \lim_{\Delta t \to 0} \left(\frac{(C_S + C)|_{t+\Delta t} - (C_S + C)|_t}{\Delta t} \right).$$

The differences in Equation 12, divided by the incremental values, define the first derivatives of $V_z C$ and Q_L with respect to z, and of $(C_S + C)$ with respect to t. Substitution of the derivatives into Equation 12 gives, upon rearrangement,

$$\frac{\partial}{\partial t} (C_S + C) = \frac{\partial}{\partial z} D_z Q_L - \frac{\partial}{\partial z} V_z C. \tag{13}$$

Since D_z and V_z are constants, subsitution for Q_L gives

$$\frac{\partial}{\partial t} C_T = D_z \frac{\partial^2}{\partial z^2} C - V_z \frac{\partial}{\partial z} C. \tag{14}$$

where C_T is the total concentration, in lb ion/ft^3 total, of ions in both phases of any increment of the resin bed, given by $(C_S + C)$.

The mass of ions in the liquid phase, M_L, is

$$M_L = V_T \varepsilon C \tag{15}$$

where

$\quad V_T$ = total volume of bed,

and

$\quad \varepsilon$ = bed porosity.

Likewise the mass in the resin phase, M_S, is

$$M_S = V_T (1 - \varepsilon) C_S. \tag{16}$$

The total mass of ions in the bed, or any incremental volume thereof, M_T, is given by the sum of the solid and liquid phase masses

$$M_T = V_T C_T = V_T \varepsilon C + V_T (1 - \varepsilon) C_S. \tag{17}$$

Equation 14 is now written in terms of masses as

$$\frac{\partial M_T}{\partial t} = D_z \frac{\partial^2 M_L}{\partial z^2} - V_z \frac{\partial M_L}{\partial z}. \tag{18}$$

Substituting Equations 15 and 17 into Equation 18 gives

$$\frac{\partial}{\partial t}(V_T \varepsilon C + V_T (1 - \varepsilon) C_S) = D_z \frac{\partial^2 (V_T \varepsilon C)}{\partial z^2} - V_z \frac{\partial (V_T \varepsilon C)}{\partial z}. \tag{19}$$

Since V_T and ε are constants, they can be brought out of the partial derivatives of Equation 19 to give

$$V_T \varepsilon \frac{\partial C}{\partial t} + V_T (1 - \varepsilon) \frac{\partial C_S}{\partial t} = D_z V_T \varepsilon \frac{\partial^2 C}{\partial z^2} - V_z V_T \varepsilon \frac{\partial C}{\partial z}. \tag{20}$$

Dividing Equation 20 by $V_T \varepsilon$ gives

$$\frac{\partial C}{\partial t} + \left(\frac{1 - \varepsilon}{\varepsilon}\right) \frac{\partial C_S}{\partial t} = D_z \frac{\partial^2 C}{\partial z^2} - V_z \frac{\partial C}{\partial z}. \tag{21}$$

According to equilibrium theory, the resin phase accumulation term, $\frac{\partial C_S}{\partial t}$, is related to the liquid pase accumulation term, $\frac{\partial C}{\partial t}$, by the equilibrium isotherm.

The isotherms to be considered in this study are the linear, Langmuir, and Freundlich isotherms. The equations of these isotherms, along with their time derivatives, are summarized in Table I.

TABLE I

EXCHANGE ISOTHERMS

Linear	Langmuir	Freundlich
$C_S = KC$	$C_S = \frac{KC}{1 + KC} C_{Smax}$	$C_S = KC^n$
$\frac{\partial C_S}{\partial t} = K \frac{\partial C}{\partial t}$	$\frac{\partial C_S}{\partial t} = \frac{KC_{Smax}}{(1 + KC)^2} \frac{\partial C}{\partial t}$	$\frac{\partial C_S}{\partial t} = nKC^{n-1} \frac{\partial C}{\partial t}$

Inserting the time derivative of the solid phase concentration into Equation 21 gives

$$\frac{\partial C}{\partial t} + \left(\frac{1 - \varepsilon}{\varepsilon}\right) f(C) \frac{\partial C}{\partial t} = D_z \frac{\partial^2 C}{\partial z^2} - V_z \frac{\partial C}{\partial z} \tag{22}$$

where $f(C)$ is the proportionality factor from the isotherm equation. Factoring $\frac{\partial C}{\partial t}$ out of Equation 22 gives the final form of the one-dimensional C-D equation to be studied

$$[1 + f(C) \, (\frac{1 - \varepsilon}{\varepsilon})] \, \frac{\partial C}{\partial t} = D_z \, \frac{\partial^2 C}{\partial z^2} - V_z \, \frac{\partial C}{\partial z} \, . \tag{23}$$

Initial and Boundary Conditions

Equation 23 contains two spatial derivatives and one time derivative. Therefore, two boundary conditions and one initial condition are required for its solution.

The most realistic initial condition defines the solution concentration at all points within the bed at time $t = 0$. Mathematically, this is written as

$$C(z,o) = C_{initial}. \tag{24}$$

The first boundary condition states that the liquid concentration at the top of the resin bed is constant and equal to the inlet solution concentration. This is written as

$$C(o,t) = C_o. \tag{25}$$

The second boundary condition concerns the concentration gradient at the bottom of the column. Physically, it requires that after a parcel of solution flows out of the bed, the exchange process is complete, and the concentration does not change further. This condition is written as

$$\frac{\partial C(L,t)}{\partial z} = 0 \ .$$

(26)

Danckwerts (1953) indicated that this was the proper boundary condition to avoid the unacceptable conclusion that the solution concentration passes through a maximum or minimum somewhere in the column.

Additional Parameters of the Model

Solution Interstitial Velocity

The average interstitial velocity of the solution, which is constant with time and distance, is given by

$$V_z = \frac{\dot{V}}{A\varepsilon}$$

(27)

where

$\dot{V}$ = solution volumetric flow rate, ft^3/sec,

A = column cross-sectional area, ft^2,

and

ε = resin bed porosity.

Axial Hydrodynamic Dispersion Coefficient

Harleman et al. (1963) reported the empirical relation for axial hydrodynamic dispersion coefficient, in beds of spherical particles, given by

$$D_{zhydro} = .66 \frac{\mu_f}{\rho_f} Re_p^{1.2} ,$$

(28)

where

μ_f = fluid viscosity, lb/ft/sec,

ρ_f = fluid density, lb/ft^3,

and

Re_p = $D_p \, V_z \, \rho_f / \mu_f$,

where

D_p = resin particle diameter.

Numerical Dispersion Coefficient

Fanchi (1983) reported equations for a numerical dispersion coefficient, D_{znum}, for use with finite-difference methods, which were based on the type of numerical representations used to approximate the partial derivatives of the equation of interest. For a centered-difference in space, explicit-in-time representation, the numerical dispersion coefficient is given by

$$D_{znum} = -\frac{1}{2} V_z^2 \frac{\Delta t}{\varepsilon} \tag{29}$$

where

V_z = average interstitial velocity, ft/sec,

Δt = time increment, sec,

and

ε = porosity.

A summary of the truncation error analysis is included in Appendix D. The overall dispersion coefficient, D_z, in Equation 23 is given by

$$D_z = D_{zhydro} - D_{znum} \tag{30}$$

where D_{znum} is subtracted to eliminate the effect of numerical dispersion on the numerical solution.

Column Pressure Drop. An expression for total pressure drop across the entire resin bed was reported by Ergun (1952) as

$$\Delta p = \frac{150 \ L \ \mu_f \ V_0 \ (1 - \varepsilon)^2}{D_p^2} + \frac{1.75 \ \rho_f \ V_0^2 \ (1 - \varepsilon)}{D_p \ \varepsilon^3 \ g_c} \tag{31}$$

where

V_0 = superficial column velocity, ft/sec,

ρ_f = fluid density, lb/ft^3,

μ_f = fluid viscosity, lb/ft/sec,

D_p = particle diameter, ft,

L = bed length, ft,

ε = bed porosity,

and

$$g_c = 32.2 \ \frac{ft \ lbm}{sec^2 lbf} \ .$$

CHAPTER IV

NUMERICAL SOLUTION OF THE
CONVECTION-DISPERSION EQUATION

This chapter has three primary functions. First, a qualitative discussion of finite-difference approximations of partial differential equations is given. Secondly, the finite-difference equations are developed based on a grid network in space and time. Finally, the solution algorithm for the system of algebraic equations generated by the implicit finite-difference method is outlined.

Description of the Finite-Difference Technique

When using a finite-difference technique, the system is first divided into a network of grid points. The distances between grid points are incremental values of the independent variables. The derivatives of the partial differential equation of interest are then written as difference equations involving the incremental values of the independent variables. Solution of the equation(s) gives the value(s) of the dependent variable at the grid points of interest. By reducing the size of the independent-variable increments, the approximation of the dependent variable approaches the true value of this variable at any grid point.

The two basic finite-difference methods are the explicit and implicit methods. The explicit finite-difference method uses known

values of the dependent variable, at previous increments of the independent variables, to predict dependent-variable values at succeeding increments. The implicit finite-difference method uses unknown values of the dependent variable, at subsequent increments of independent variables, to predict dependent-variable values at succeeding increments. The equations generated for the entire incremental level must be solved simultaneously by solving a matrix of coefficients. This matrix solution yields an entire incremental level of dependent-variable values.

The method used in the present work is the implicit method. This insures numerical stability at all values of Δz and Δt.

Formulation of the Finite-Difference Equations. Derivation of the finite-difference equations requires division of the ion-exchange resin bed into spatial increments of thickness Δz. Figure 2 is a representation of the discrete element system. Distance increments are subscripted i, and the distance increment Δz, is equal to $(z_{i+1} - z_i)$. Time, subscripted j, is the other coordinate of the grid, and the temporal increment Δt is equal to $(t_{j+1} - t_j)$.

Following the development of Laumbach (1975), finite-difference approximations for the partial derivatives in Equation 14 are obtained by Taylor series expansion of concentration about the ith spatial node, and any temporal node, such that

$$C_{i+1} = C_i + \Delta z \left.\frac{\partial C}{\partial z}\right|_i + \frac{(\Delta z)^2}{2} \left.\frac{\partial^2 C}{\partial z^2}\right|_i + \frac{(\Delta z)^3}{3!} \left.\frac{\partial^3 C}{\partial z^3}\right|_i + \cdots \qquad (32)$$

and
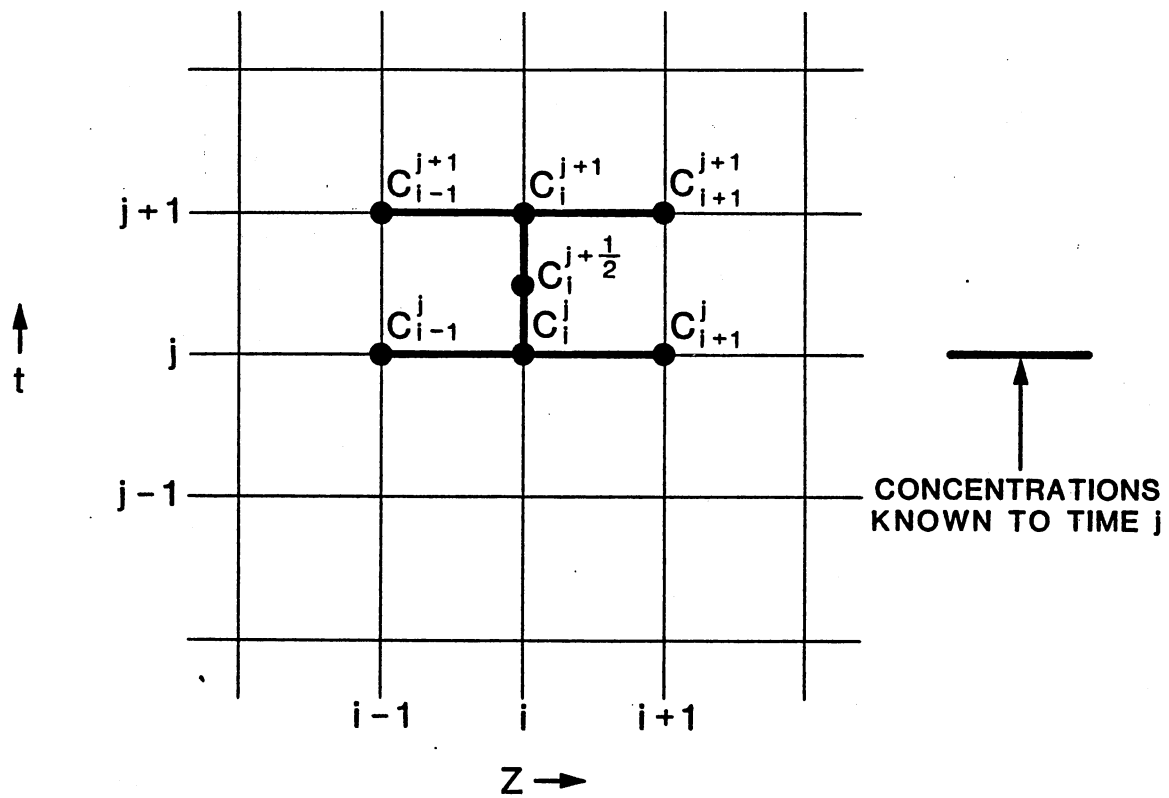
Figure 2. Arrangement of Finite-Difference Grid

$$C_{i-1} = C_i \mp \Delta z \left.\frac{\partial C}{\partial z}\right|_i + \frac{(\Delta z)^2}{2} \left.\frac{\partial^2 C}{\partial z^2}\right|_i - \frac{(\Delta z)^3}{3!} \left.\frac{\partial^3 C}{\partial z^3}\right|_i + \ldots \quad (33)$$

Adding Equations 32 and 33 gives

$$\frac{1}{2}(C_{i+1} + C_{i-1}) = C_i + \frac{(\Delta z)^2}{2} \left.\frac{\partial^2 C}{\partial z^2}\right|_i + \frac{(\Delta z)^4}{4!} \left.\frac{\partial^4 C}{\partial z^4}\right|_i + \ldots \quad (34)$$

Equation 34 is now differentiated once with respect to time to give

$$(35)$$

$$\left.\frac{\partial C}{\partial t}\right|_i = \frac{1}{2}\left(\left.\frac{\partial C}{\partial t}\right|_{i+1} + \left.\frac{\partial C}{\partial t}\right|_{i-1}\right) - \frac{(\Delta z)^2}{2} \frac{\partial^3 C}{\partial t \partial z^2} - \frac{(\Delta z)^4}{4!} \frac{\partial^5 C}{\partial t \partial z^4} + \ldots$$

C is now expanded about the $j + \frac{1}{2}$ temporal node to give the approximations

$$(36)$$

$$C_i^{j+1} = C_i^{j+\frac{1}{2}} + \frac{\Delta t}{2} \left.\frac{\partial C}{\partial t}\right|_i^{j+\frac{1}{2}} + \frac{(\Delta t)^2}{8} \left.\frac{\partial^2 C}{\partial t^2}\right|_i^{j+\frac{1}{2}} + \frac{(\Delta t)^3}{48} \left.\frac{\partial^3 C}{\partial t^3}\right|_i^{j+\frac{1}{2}} + \ldots$$

and

$$(37)$$

$$C_i^j = C_i^{j+\frac{1}{2}} - \frac{\Delta t}{2} \left.\frac{\partial C}{\partial t}\right|_i^{j+\frac{1}{2}} + \frac{(\Delta t)^2}{8} \left.\frac{\partial^2 C}{\partial t^2}\right|_i^{j+\frac{1}{2}} - \frac{(\Delta t)^3}{48} \left.\frac{\partial^3 C}{\partial t^3}\right|_i^{j+\frac{1}{2}} + \ldots$$

Subtracting Equation 37 from Equation 36 gives, upon rearrangement,

$$\left.\frac{\partial C}{\partial t}\right|_i^{j+\frac{1}{2}} = \frac{C_i^{j+1} - C_i^j}{\Delta t} + \frac{(\Delta t)^2}{4} \left.\frac{\partial^3 C}{\partial t^3}\right|_i^{j+\frac{1}{2}} + \ldots \quad (38)$$

Neglecting derivatives of order two and higher gives an approximation for the accumulation term in Equation 23.

$$\frac{\partial C}{\partial t} = \frac{C_i{'} - C_i}{\Delta t} + \Theta(\Delta t^2) \tag{39}$$

where

$$C_i{'} = C_i^{j+1}$$
$$C_i = C_i^{j}$$

and

Θ = "order of error."

The approximation of the first-order spatial derivative is formed by subtracting Equation 33 from Equation 32 to give

$$\frac{\partial C}{\partial z}\bigg|_i = \frac{C_{i+1} - C_{i-1}}{2\Delta z} - \frac{(\Delta z)^2}{6}\frac{\partial^3 C}{\partial z^3} + \ldots \tag{40}$$

Equations 36 and 37 are added to give

$$\frac{1}{2}(C_i{'} + C_i) = C_i^{j+\frac{1}{2}} + \frac{(\Delta t)^2}{8}\frac{\partial^2 C}{\partial t^2}\bigg|_i^{j+\frac{1}{2}} + \ldots \tag{41}$$

Substituting Equation 39 into the appropriate derivatives of Equation 41, and neglecting derivatives of order two and higher, gives the approximation for the convection term of Equation 23,

$$\frac{\partial C}{\partial z}\bigg|_i^{j+\frac{1}{2}} = \frac{1}{4\Delta z}(C_{i+1}{'} - C_{i-1}{'} + C_{i+1} - C_{i-1}) + \Theta(\Delta z^2), \tag{42}$$

The approximation of the second-order spatial derivative is developed from the sum of Equations 32 and 33, given by

$$\frac{\partial^2 C}{\partial z^2}\bigg|_i = \frac{C_{i+1} - 2C_i + C_{i-1}}{(\Delta z)^2} - \frac{(\Delta z)^2}{12}\frac{\partial^4 C}{\partial z^4}\bigg|_i + \cdots \cdots \tag{43}$$

Differentiating Equation 41 twice with respect to z, and rearranging the results, gives

$$\frac{\partial^2 C}{\partial z^2}\bigg|_i^{j+\frac{1}{2}} = \frac{1}{2}\left(\frac{\partial^2 C}{\partial z^2}\bigg|_i^{j+1} + \frac{\partial^2 C}{\partial z^2}\bigg|_i^{j}\right) - \frac{(\Delta t)^2}{8}\frac{\partial^4 C}{\partial z^2 \partial t^2}\bigg|_i^{j+\frac{1}{2}} + \cdots \cdots \tag{44}$$

Substituting Equation 43 into the appropriate derivatives of Equation 44, and neglecting derivatives of order two and higher, gives the aproximation for the dispersion term of Equation 23,

$$\tag{45}$$

$$\frac{\partial^2 C}{\partial z^2}\bigg|_i^{j+\frac{1}{2}} = \frac{1}{2(\Delta z)^2}(C'_{i+1} - 2C'_i + C'_{i-1} + C_{i+1} - 2C_i + C_{i-1}) + \Theta(\Delta z^2)$$

The order of truncation error in Equation 45 is consistent with the orders of error in the other two approximating equations, namely Equations 39 and 42.

Substituting Equations 45, 39, and 42 into the appropriate terms of Equation 23 gives the finite-difference approximation of the C-D equation

$$\frac{1}{\Delta t}\left[1 + f(C)\left(\frac{1-\epsilon}{\epsilon}\right)\right](C'_i - C_i) \tag{46}$$

$$= \frac{D_z}{2(\Delta z)^2}(C'_{i+1} - 2C'_i + C'_{i-1} + C_{i+1} - 2C_i + C_{i-1})$$

$$- \frac{V_z}{4\Delta z}(C'_{i+1} - C'_{i-1} + C_{i+1} - C_{i-1}).$$

Defining parameters

$$Q = \frac{1}{\Delta t} [1 + f(C)(\frac{1 - \varepsilon}{\varepsilon})],$$

$$R = \frac{D_z}{2(\Delta z)^2},$$

and

$$S = \frac{V_z}{4\Delta z},$$

and substituting these parameters into Equation 46 gives, after rearranging, the general difference analogue to Equation 23

$$(-R-S)\ C'_{i-1} + (Q + 2R)\ C'_i + (-R + S)\ C'_{i+1} \tag{47}$$

$$= (R + S)\ C_{i-1} + (Q - 2R)\ C_i + (R - S)\ C_{i+1}.$$

Equation 47 is written for every spatial node at each time step. The system of equations which is generated for the time step is given, in Table II, by Equation 48.

TABLE II

FINITE-DIFFERENCE EQUATIONS

$$(Q + 2R)\ C'_1 + (-R - S)\ C'_2 = T_1$$
$$(-R - S)\ C'_1 + (Q + 2R)\ C'_2 + (-R + S)\ C'_3 = T_2$$
$$(-R - S)\ C'_2 + (Q + 2R)\ C'_3 + (-R + S)\ C'_4 = T_3$$

$$\cdots$$

$$\cdots \qquad (48)$$

$$\cdots$$

$$(-R - S)\ C'_{N-2} + (Q + 2R)\ C'_{N-1} + (-R - S)\ C'_N = T_{N-1}$$
$$(-R - S)\ C'_{N-1} + (Q + R + S)\ C'_N = T_N,$$

where

$$T_i = (-R - S)\ C'_0 + (R + S)\ C_0 + (Q - 2R)\ C_1 + (R - S)\ C_2,\ i=1,$$
$$T_i = (R + S)\ C_{i-1} + (Q - 2R)\ C_i + (R - S)\ C_{i+1},\ 2 \leqslant i \leqslant N-1,$$
$$T_i = (R + S)\ C_{i-1} + (Q - R - S)\ C_i,\ i = N.$$

When nonlinear isotherms are used in evaluation of the model, $f(C)$ is not a constant. This difficulty is avoided by assuming $f(C)$ to be constant over any spatial increment, and evaluating $f(C)$ based on solution concentration within the increment. This procedure linearizes Equation 23 over any incremental slice of the column.

The individual equations of Equation 48 are of the form

$$A_i S_{i-1} + B_i S_i + C_i S_{i+1} = D_i. \tag{49}$$

The Gaussian elimination algorithm used to solve the diagonally-dominant system of equations of the form of Equation 49 is summarized below.

$$S_i = \gamma_i - \frac{C_i S_{i+1}}{\beta_i}, \quad 1 \leqslant i \leqslant N-1, \tag{50}$$

$$S_N = \gamma_N,$$

where

$$\beta_1 = B_1,$$

$$\gamma_1 = \frac{D_1}{\beta_1},$$

$$\beta_i = B_i - \frac{A_i C_{i-1}}{\beta_{i-1}}, \quad 2 \leqslant i \leqslant N,$$

and

$$\gamma_i = \frac{D_i - A_i \gamma_{i-1}}{\beta_i}, \quad 2 \leqslant i \leqslant N.$$

CHAPTER V

RESULTS

This chapter presents an evaluation of the model proposed in
Chapters III and IV. Calculations using the model are compared to a
closed-form analytical solution and to experimental data involving both
linear and nonlinear equilibrium isotherms.

Model Evaluation

The finite-difference algorithm, the core of which was given by
Equation 48 and the solution algorithm of Chapter IV has been
incorporated into an interactive computer program, a listing of which is
given in Appendix A. The program was developed on a Radio Shack TRS 80
Model II Microcomputer, and tested on the VAX 11/780 of the Oklahoma
State University Computer Center Network.

The validity of the numerical solution was verified by test runs
with data for a system which was described by a linear equilibrium
isotherm. The results from these runs were compared with the results of
evaluation of the analytical solution given by Equation 9. The
parameters of the model were then adjusted to match experimental
breakthrough data for several systems which were described by linear and
nonlinear equilibria.

Finally, sensitivity tests were conducted to determine the effect
of changes in four system parameters on the numerical solution. The

parameters chosen for this analysis were spatial increment size, temporal increment size, bed porosity, and equilibrium constant.

A material balance check calculation was performed for the linear system described above. In 800 seconds of simulation time, the error in total mass balance was 0.0227 lb/ft^3. This gives a percentage error of approximately 1.0%. Pressure drop calculations matched the values of Dow Chemical Company (1964), for their ion exchange resins, to within 0.5 psi.

Discussion of Results

Figure 3 is a plot of the analytical and numerical solutions of Equation 23. Partial removal of numerical dispersion from the numerical solution is evidenced by improvement in the agreement between the analytical and numerical solutions upon the inclusion of D_{znum} in the model.

For the data of Appendix C, the experimentally determined column performance data from the literature and the numerical data predicted by the proposed model are compared graphically in Figures 4, 5, and 6. These figures represent the best agreement, obtained from model parameter adjustment, of predicted data with experimental data for a linear system, an unfavorable nonlinear system, and a favorable nonlinear system, respectively.

Adjustment of ε produced the best agreement between predicted and experimental data for all three systems studied. Since ε affects the value of both convective and dispersive parameters, a change in its value changes both the breakthrough time and the shape of the breakthrough curve. Additionally, adjustment of ε is reasonable since
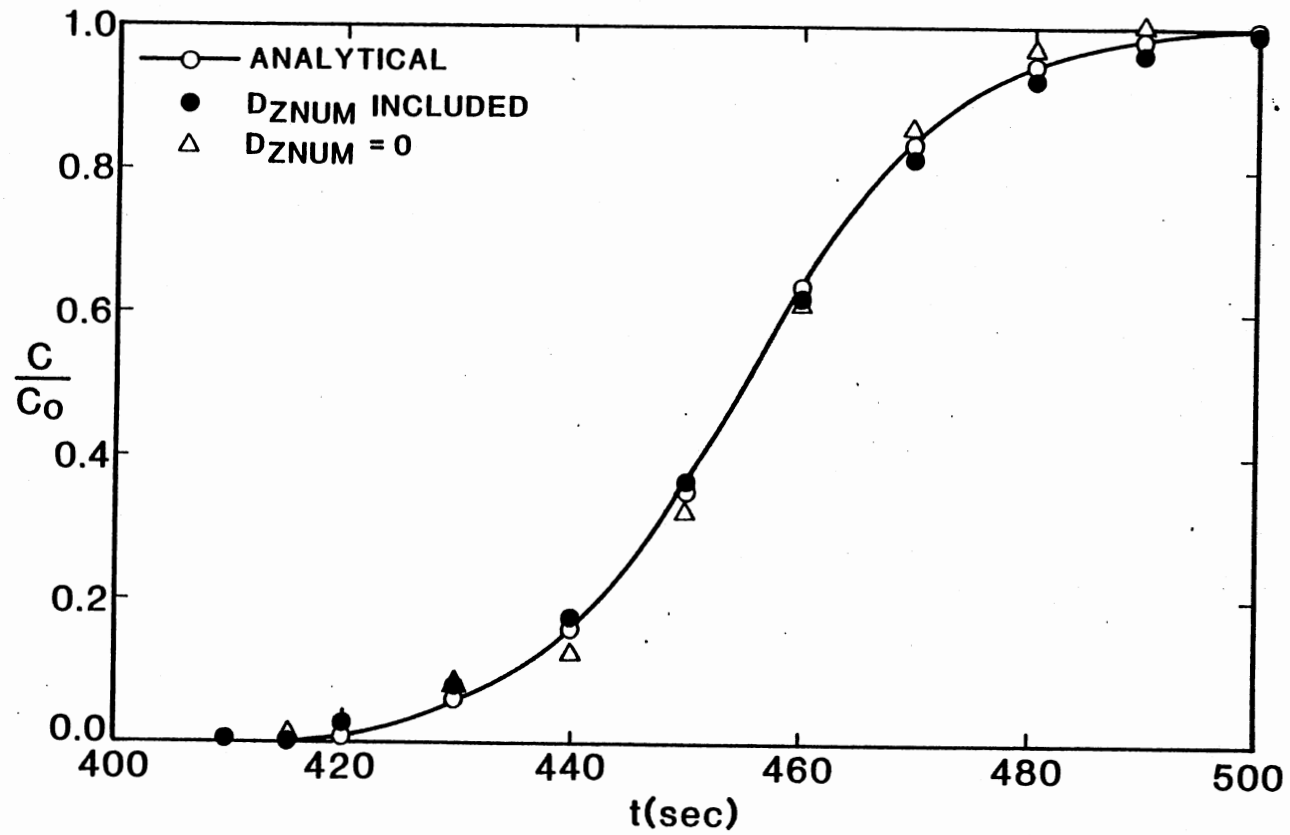
Figure 3. Comparison of Analytical and Numerical Solutions
to the Linear, One-Dimensional Convection-
Dispersion Equation.
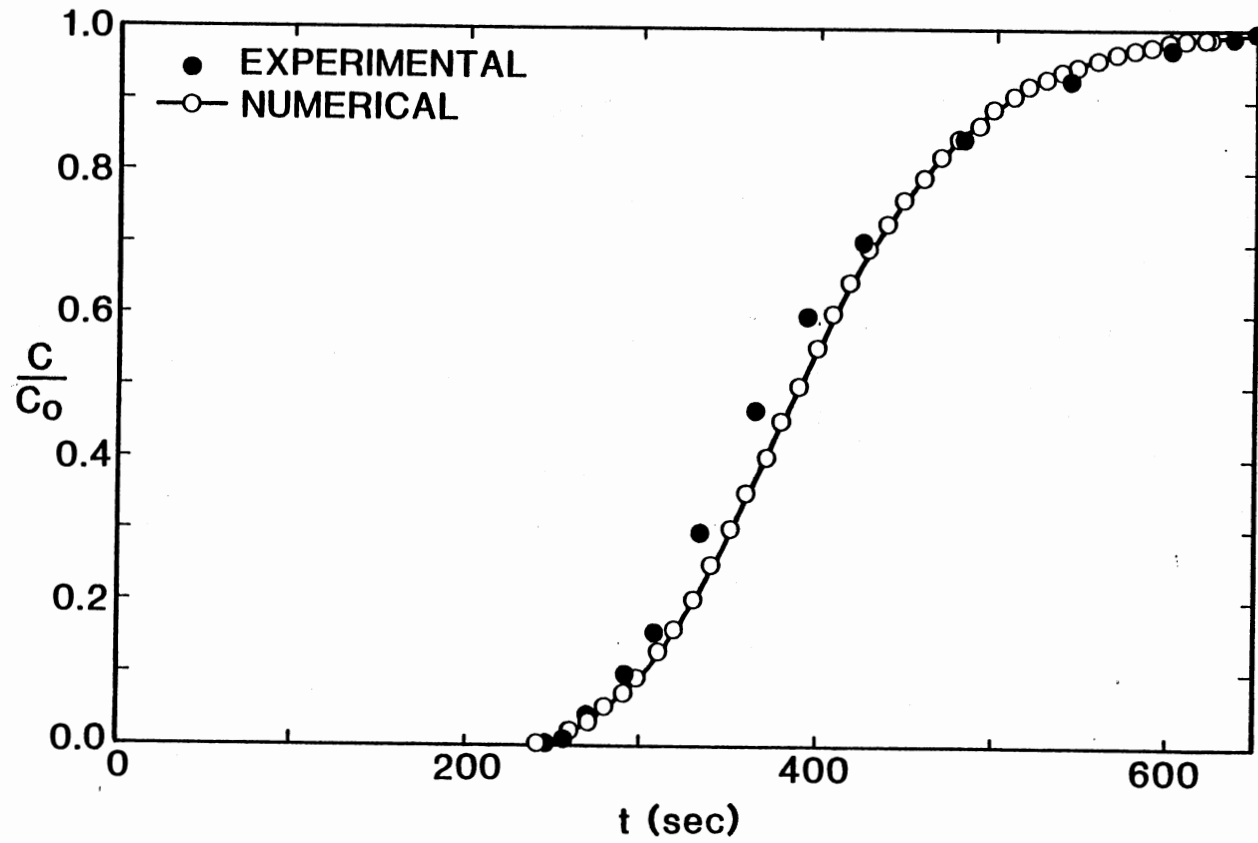
Figure 4.   Comparison of Experimental and Numerical Data;
Linear Isotherm, Δz=0.023 Ft., Δt=1.0 Second,
G=0.2, Fk=0.58.
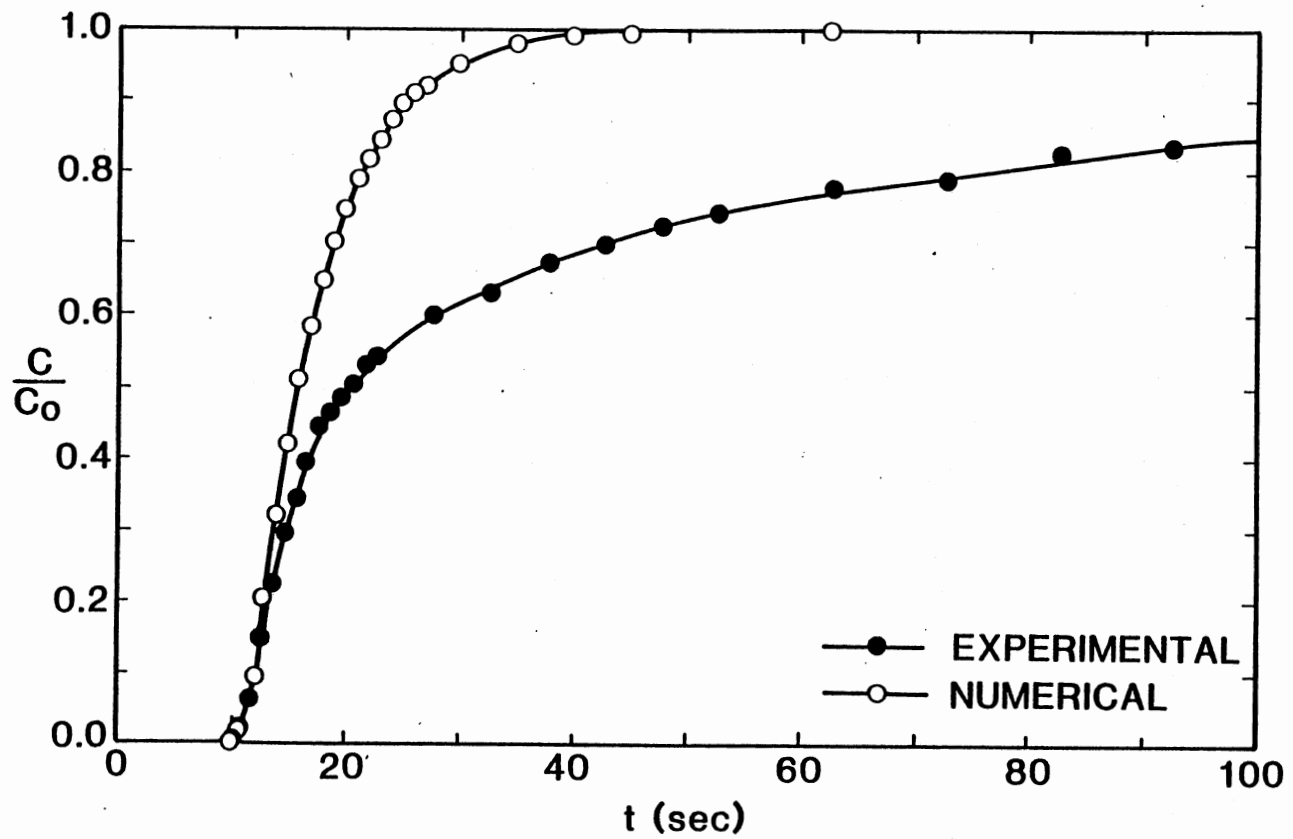
Figure 5. Comparison of Experimental and Numerical Data;
Freundlich Isotherm, Unfavorable Exchange,
Δz=0.017Ft., Δt=1.0 Second, ϵ=0.3, Fk=1.117,
Fn=0.4447.

Figure 6. Comparison of Experimental and Numerical Data;
Freundlich Isotherm, Favorable Exchange,
$\Delta z = 0.017$ Ft., $\Delta t = .01$ Second, $\epsilon = 0.15$, $Fk = 1.117$,
$Fn = 0.4447$.

local porosities within the resin bed cover a range of values due to the randomness of the particle arrangement. The typical range of porosity for beds of spherical particles is 0.2 - 0.4.

Subtraction of additional numerical dispersion, through a larger value of Δt, produced an additional benefit. The value of D_z was increased, through subtraction of the increased negative value of D_{znum}, so that overshoot and oscillation were eliminated from the predicted breakthrough curve. The increased value of D_z also improved the agreement between predicted and experimental data.

Figure 4 shows agreement between predicted and experimental data over the entire breakthrough curve. Figures 5 and 6 show that the predicted breakthrough time matches the experimental breakthrough time for favorable and unfavorable systems. However, the curve is more closely approached for the unfavorable equilibrium system.

Ion exchange under low solution flow rate conditions is more closely approximated by equilibrium theory than is exchange under conditions of high solution flow rate. The flow rates of the nonlinear systems are over 100 times greater than the linear system flow rate. Therefore, the closer agreement with the linear data is primarily due to a lower solution flow rate. The closer approach of the unfavorable exchange system is due to the nonsharpening boundary observed under unfavorable exchange conditions. The column operates closer to equilibrium under these conditions.

The four parameters chosen for sensitivity tests were spatial increment, Δz, temporal increment, Δt, porosity, ϵ, and linear equilibrium constant, F_k. Table III gives the values of each parameter used in the numerical sensitivity tests, the graphical results of which

are presented in Figures 7 through 14. For comparative purposes, the
tests were run both with and without the inclusion of the numerical
dispersion coefficient, D_{znum}.

TABLE III

SENSITIVITY TESTS

Fig. #	Δz (ft)	Δt (sec)	ε	F_k	D_{znum}
7	0.008-0.023	1.0	0.4	0.58	yes
8	0.008-0.023	1.0	0.4	0.58	no
9	0.023	0.01-1.0	0.4	0.58	yes
10	0.23	0.01-1.0	0.4	0.58	no
11	0.023	1.0	0.3-0.4	0.58	yes
12	0.023	1.0	0.3-0.4	0.58	no
13	0.023	1.0	0.4	0.55-0.65	yes
14	0.023	1.0	0.4	0.55-0.65	no

Dependence of Predicted Data on Δz

Comparison of Figures 7 and 8 shows well how the inclusion of the
numerical dispersion coefficient eliminated the dependence of predicted
data on Δz. Without the numerical dispersion coefficient, V_z was
approximately 100 times larger than D_z. The increased hyperbolic nature
of the C-D equation under this condition explains the overshoot observed

Figure 7. Numerical Results of Δz Sensitivity Tests With Numerical Dispersion Coefficient Included.

Figure 8. Numerical Results of Δz Sensitivity Tests With Numerical Dispersion Coefficient Excluded.

in Figure 8. With numerical disperison subtracted from the model, V_z was approximately 10 times larger than D_z, which caused the C-D equation to become more parabolic and eliminated overshoot in the predicted breakthrough curve. From Figure 8, a decreased Δz, which corresponded to more spatial increments, lessened the overshoot and sharpened the curve.

Dependence of Predicted Data on Δt

Figures 9 and 10 show the effect of changes in the value of Δt on the numerical solution with and without numerical dispersion accounted for. Opposite to the dependence of Δz, subtraction of D_{znum} from the model resulted in sensitivity to the value of Δt, while exclusion of D_{znum} from the model resulted in no appreciable effect of Δt. This result was due to the fact that D_{znum} is directly proportional to the value of Δt (see Equation 29). Therefore, a decrease in Δt caused a decrease in D_{znum}, with an increase in the difference between V_z and D_z. Increased hyperbolic character of the C-D equation appears, in Figure 9, as sharpened the breakthrough curve, due to a smaller dispersive term in the C-D equation.

Dependence of Predicted Data on ε

This parameter was chosen for sensitivity tests because of the questionable, but unavoidable, assumption of a homogeneous resin bed with constant porosity throughout. The effective porosity will probably be lower than the normally reported of 0.35 - 0.40, due to the presence of dead pore volume which contains stagnant solution, and nonhomo-geneities resulting from the randomness of the packing.
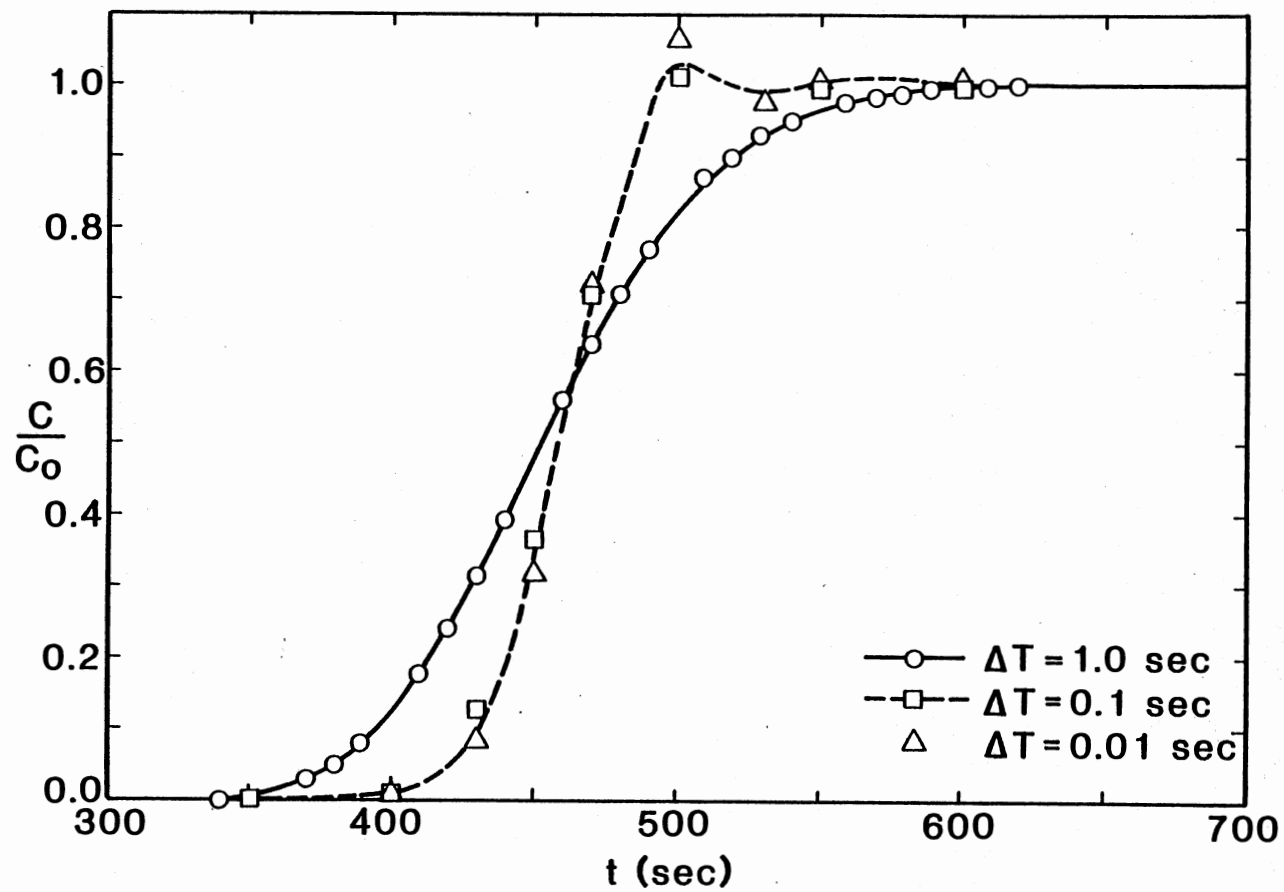
Figure 9. Numerical Results of Δt Sensitivity Tests With
Numerical Dispersion Coefficient Included.
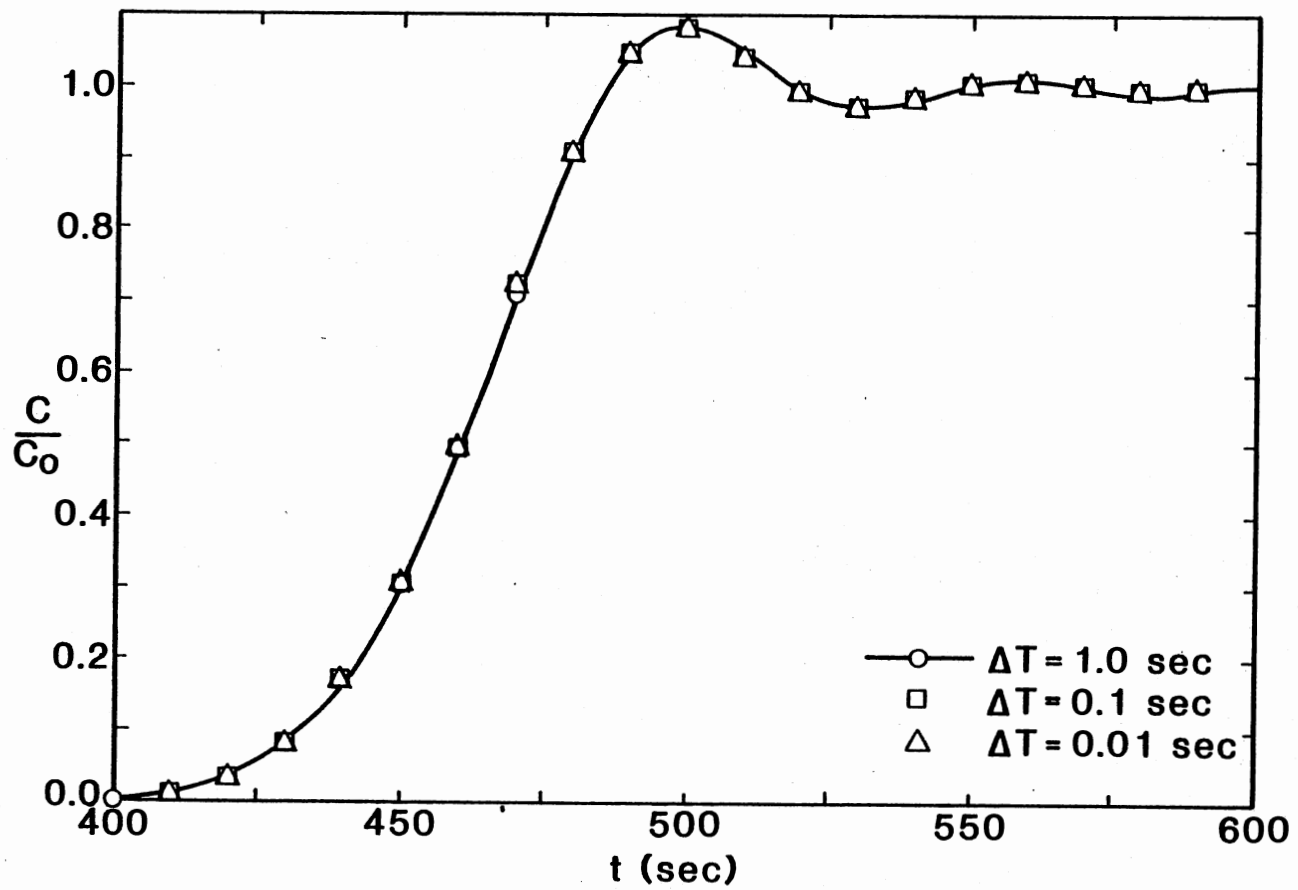
Figure 10.   Numerical Results of Δt Sensitivity Tests With
Numerical Dispersion Coefficient Excluded.

Figure 12 shows that, for the model without D_{znum}, a decrease in ε shifted the breakthrough curve ahead in time. The shape of the curve, however, was essentially unchanged.

Figure 11 shows that, with D_{znum} included in the model, the shape of the predicted curve, as well as the breakthrough time, was changed with a change in the value of ε. This was due to the fact that ε affects several parameters of the model.

From Equation 27, V_z is inversely proportional to ε. From Equation 29, D_{znum} is proportional to V_z, and inversely proportional to ε. Equation 28 indicates that D_{zhydro}, which is a function of V_z, is affected by ε. Therefore, as ε decreases, V_z, D_{znum}, and D_{zhydro} increase. Increased velocity was shown as decreased breakthrough time, while the shape of the breakthrough curve was changed due to a larger dispersive term.

Dependence of Predicted Data on F_k. This parameter was chosen for sensitivity tests due to the potential difficulties encountered in describing a set of equilibrium data by a unique constant.

Figures 13 and 14 show that a lower value of F_k shifted the breakthrough curve ahead in time. This is because the lower value of F_k effectively put more solute in the solution phase than a higher F_k value (see Table I: linear isotherm). The exchange can be said to occur more quickly throughout the column.
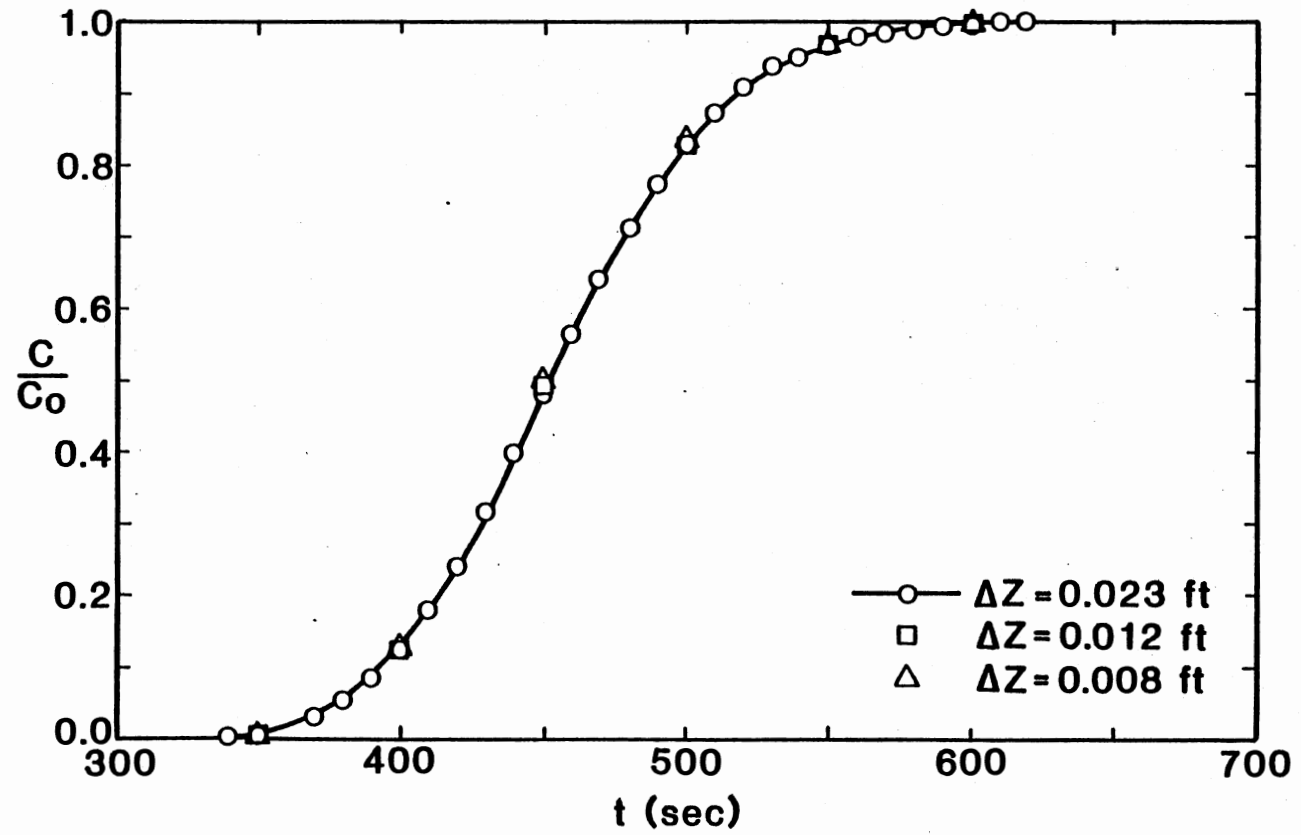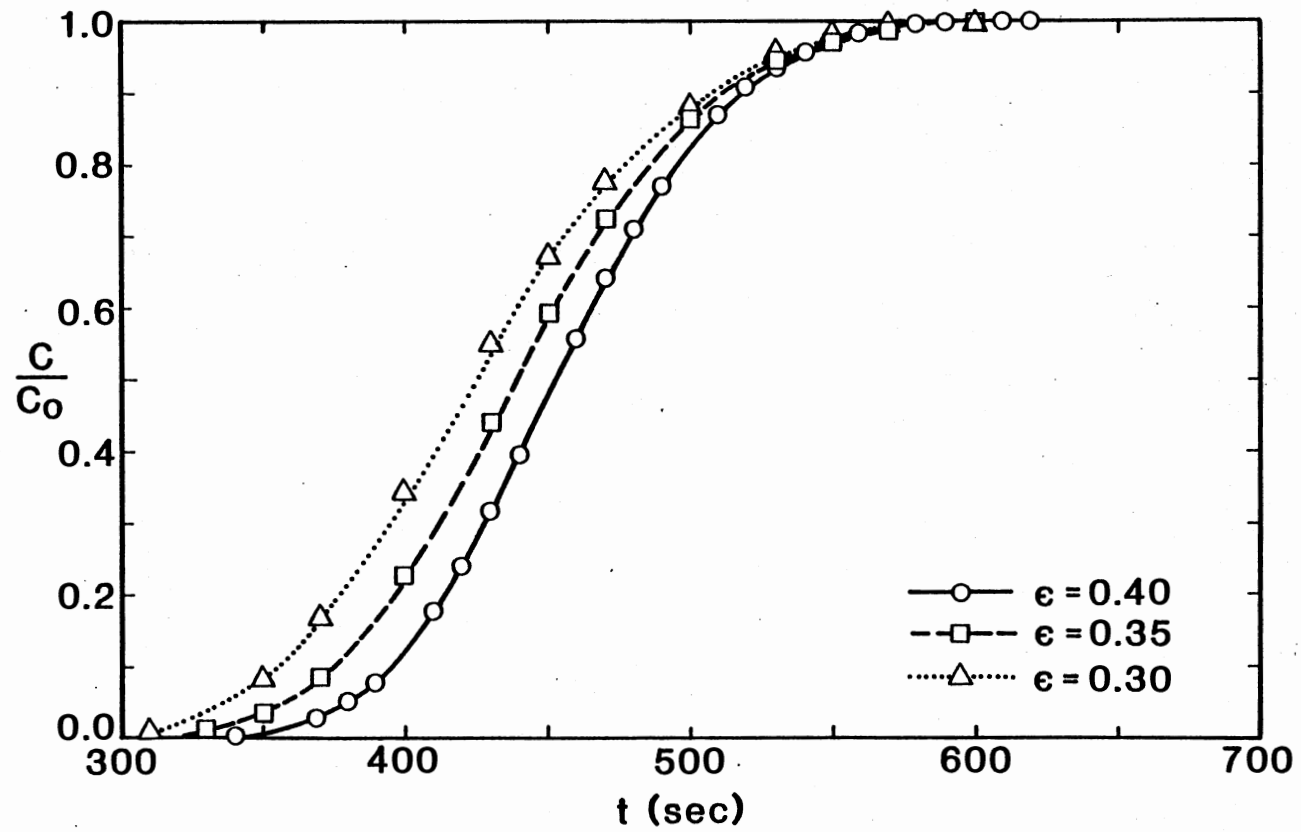
Figure 11. Numerical Results of ε Sensitivity Tests With
Numerical Dispersion Coefficient Included.

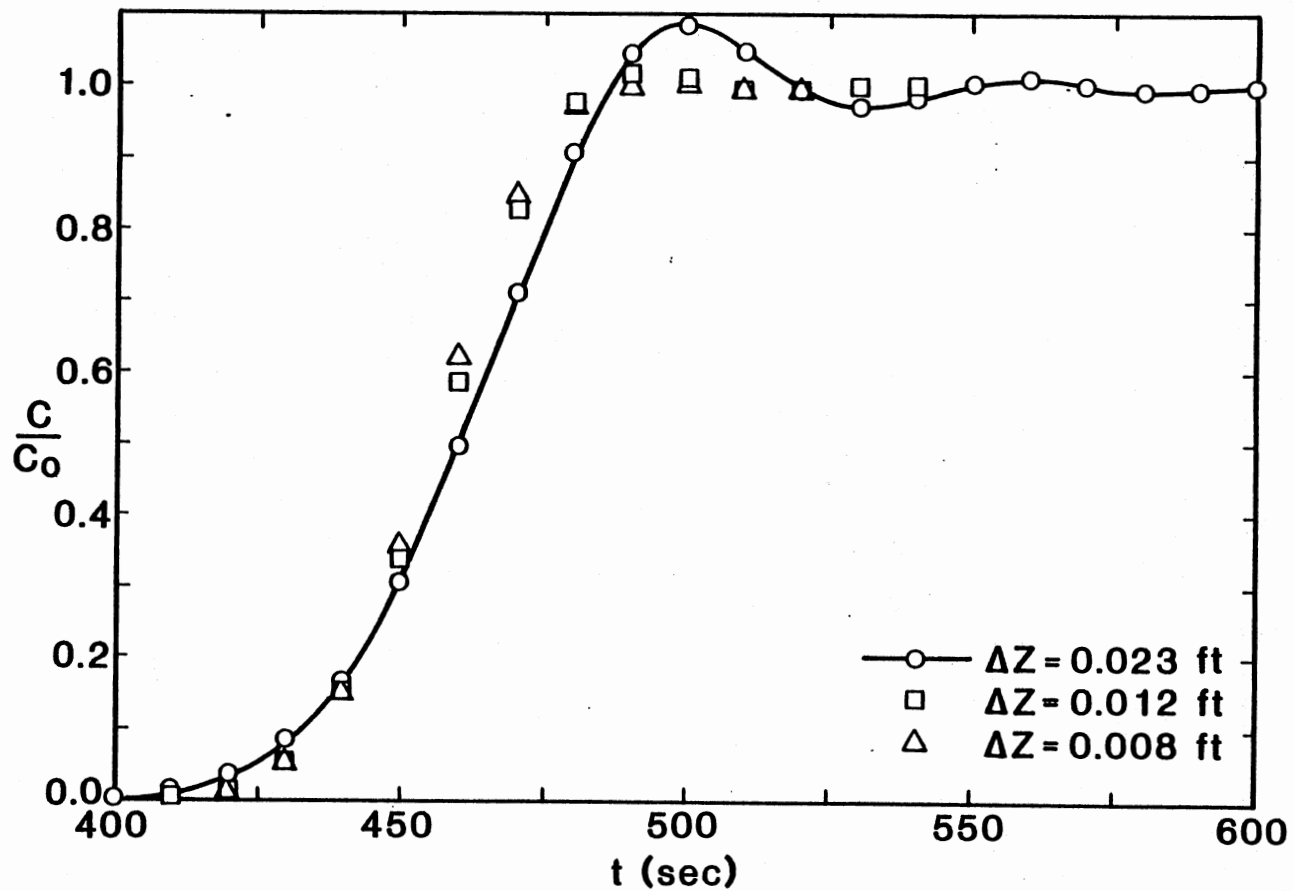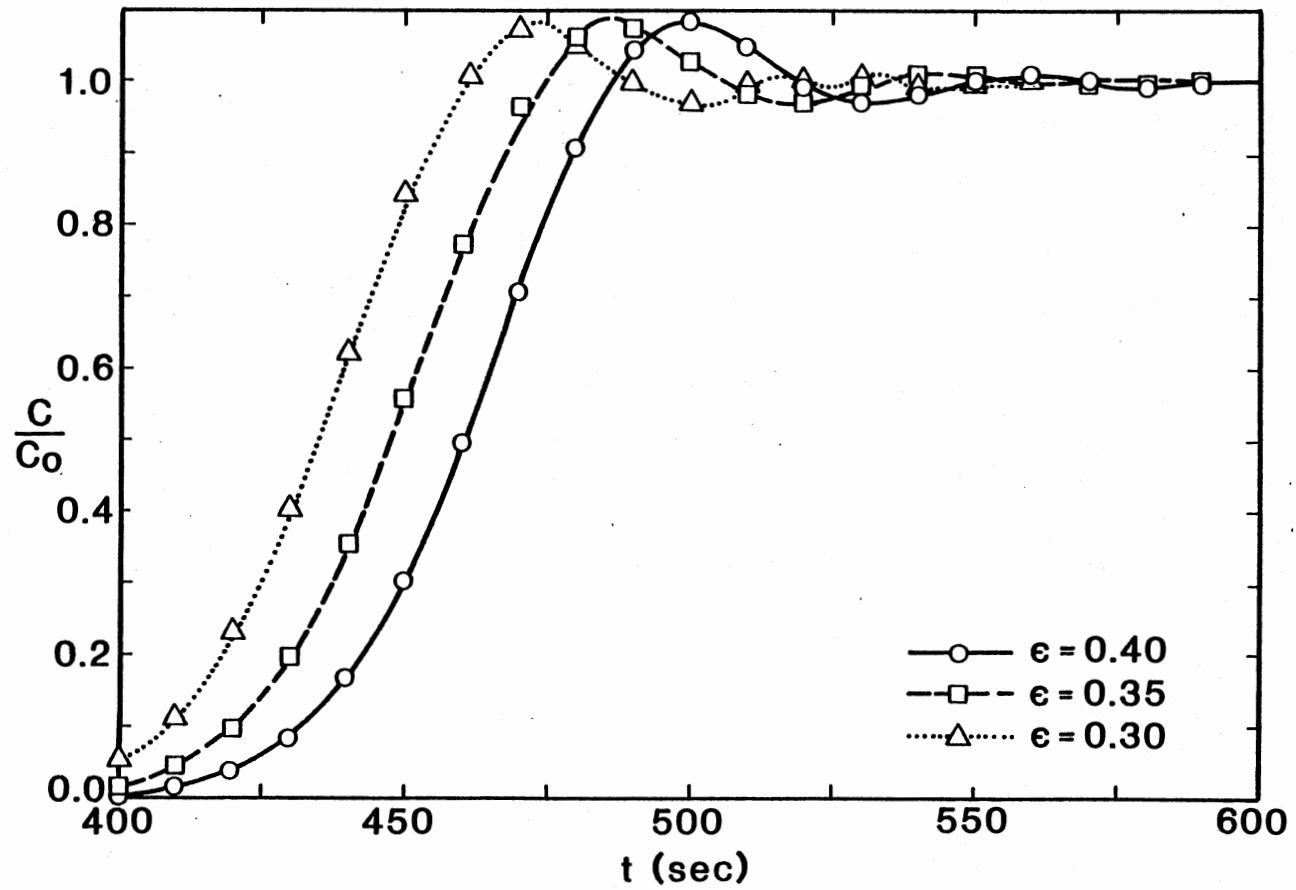Figure 12. Numerical Results of ϵ Sensitivity Tests With
Numerical Dispersion Coefficient Excluded.
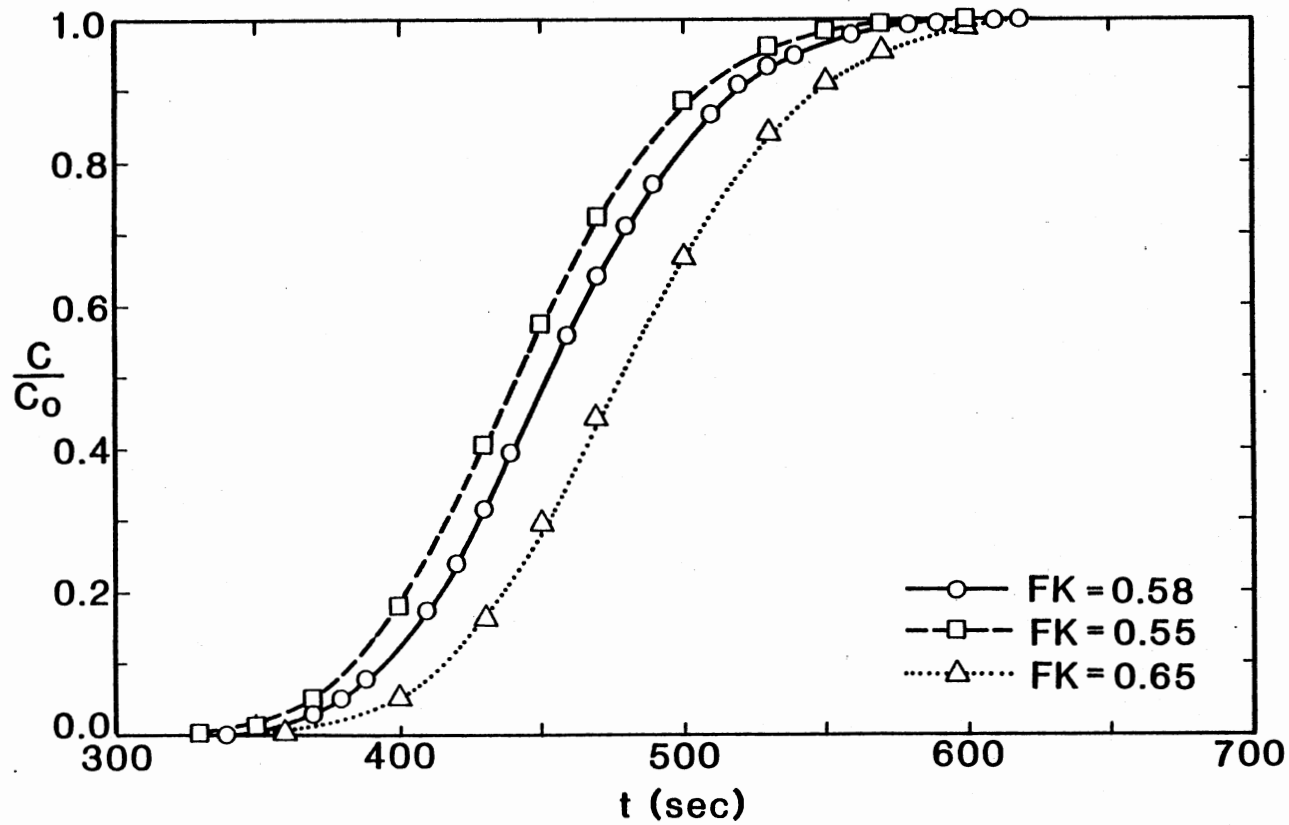
Figure 13. Numerical Results of Fk Sensitivity Tests With
Numerical Dispersion Coefficient Included.
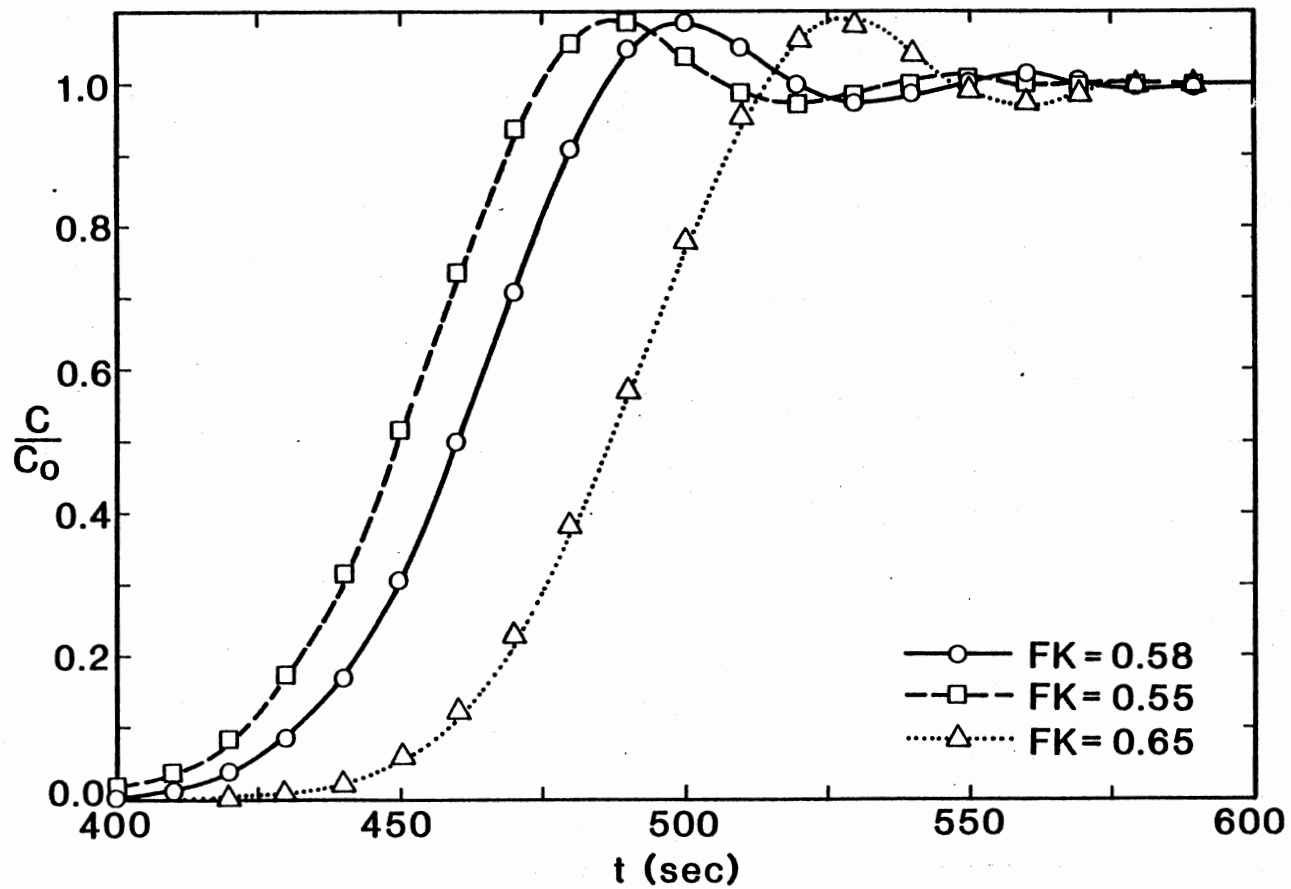
Figure 14. Numerical Results of Fk Sensitivity Tests With
Numerical Dispersion Coefficient Excluded.

CHAPTER VI

CONCLUSIONS AND RECOMMENDATIONS

Conclusions

The proposed model has several favorable features which justify its use for making operational and design decisions.

(1) Subtraction of D_{znum}, which represents error in the solution introduced by numerical dispersion, improves agreement between the numerically approximated and exact solutions. Additionally, increased subtraction of numerical dispersion eliminates overshoot from the solution and allows prediction of breakthrough curves which match actual systems.

(2) The usefulness of equilibrium theory of ion exchange is exhibited by the accuracy of breakthrough data prediction obtained without determination of the kinetic parameters of ion exchange, which can be done only through extensive experimentation for a particular system.

(3) The proposed model is applicable to general ion exchange systems with only equilibrium and column data needed for evaluation.

(4) The primary model sensitivities lie in Δt and ϵ.

(5) Adjustment of model parameters gave agreement with the breakthrough curve in certain systems and with breakthrough time in all systems studied.

(6) The computer program, which is based on an implicit finite-difference technique, is not prohibitively expensive in execution time or storage.

(7) Closure of the material balance calculation indicates lack of significant roundoff or machine errors.

Recommendations

The proposed model appears to have merit in applicability to a wide variety of ion exchange systems with a minimum of experimental data required for evaluation. The following recommendations are presented.

(1) For the systems studied in the present work, base values of 100 spatial increments, $\Delta t = 1.0$ second, and a value of porosity somewhat less than the reported values of 0.35 - 0.40 produced the best results.

(2) Although the finite-difference algorithm is stable at all values of Δt and Δz, reduction in Δt below 0.1 second and spatial increments below 50 resulted in overshoot and oscillation in the solution due to increased hyperbolic behavior of the C-D equation.

(3) Porosity, ε, is recommended as the best parameter for adjustment, since a change in ε changes the breakthrough time as well as the shape of the breakthrough curve.

(4) Parameters should be adjusted independently. Base values should be chosen for all parameters, with single parameter variations made holding other values constant.

BIBLIOGRAPHY

Brenner, H. 1962. "The Diffusion Model of Longitudinal Mixing in Beds of Finite Length. Numerical Values." Chem. Engr. Sci., 17, 229-243.

Crank, J., P. Nicolson. 1947. "A Practical Method for Numerical Evaluation of Solutions of Partial Differential Equations of the Heat-Conduction Type." Proc. Cambridge Phil. Soc., 43, 50-67.

Danckwerts, P. C. 1953. "Continuous Flow Systems, Distribution of Residence Times." Chem. Engr. Sci., 2, 1-13.

DeVault, D. 1943. "The Theory of Chromatography." J. Amer. Chem. Soc., 65, 532-540.

Dow Chemical Company. 1964. Dowex: Ion Exchange, 18.

Ergun, S. 1952. "Fluid Flow Through Packed Columns." Chem. Engr. Prog., 48, 89.

Erickson, K. L., H. F. Rase. 1979. "Fixed-Bed Ion Exchange with Differing Ionic Mobilities and Nonlinear Equilibria." Ind. Eng. Chem. Fund., 18, 4, 312-317 (also Dissertation, The University of Texas, Austin, 1977.)

Fanchi, J. R. 1983. "Multidimensional Numerical Dispersion." Soc. Pet. Eng. J., February, 143-151.

Frisch, N. W., F. X. McGarvey. 1959. "Application of Ion Exchange Equilibrium Relationships to Process Design." Chem. Engr. Prog. Symp. Ser, Vol. 55, No. 24, 51-59.

Gardner, A. O., Jr., D. W. Peaceman, A. L. Pozzi, Jr. 1964. "Numerical Calculation of Multidimensional Miscible Displacement by the Method of Characteristics." Soc. Pet. Eng. J., March, 26-36.

Glueckauf, E. 1947. "Theory of Chromatography. Parts II, III, IV, V." J. Chem. Soc., 1302-1329.

Glueckauf, E. 1955. "Principles of Operation of Ion-Exchange Columns." Ion Exchange and Its Applications. Soc. Chem. Ind., 34-36.

Harleman, D. R. F., P. F. Mehlhorn, R. R. Rumer, Jr. 1963.
"Dispersion-Permeability Correlation in Porous Media." J. Hydraul.
Div., Proc. Am. Soc. Civ. Eng., March, 67-85.

Helfferich, F. 1962. Ion Exchange, McGraw Hill, New York.

Hunt, B. 1978. "Dispersive Sources in Uniform Groundwater Flow." J.
Hydraul. Div., Proc. Am. Soc. Civ. Eng., January, 75-85.

Klein, G., K. M. Makar, B. W. Tleimat, T. Vermeulen. 1968. Design and
Cost of Ion-Exchange Softening for a 50-MGD Sea-Water Evaporation
Plant. Richmond, California, Sea Water Conversion Laboratory,
Report No. 98-2, Sepetember.

Klein, G., D. Tondeur, T. Vermeulen. 1965. Multicomponent Ion Exchange
in Fixed Beds Operated Under Equilibrium Conditions. Part I.
General Properties of Uniformly Presaturated Beds Receiving Feed of
Constant Composition. Richmond, California, Sea Water Conversion
Laboratory, Report No. 65-3, June. (also Ind. Eng. Chem. Fund.,
6,3 (1967), 339-351).

Klein, G., T. Vermeulen. 1974. Multicomponent Fixed-Bed Ion
Exchange: Theory, Practical Simplifications and Process
Applications. Richmond, California, Report No. 74-1, July.

Klein, G., M. Villena, T. Vermeulen. 1963. Removal of Scale-Forming
Constituents from Saline Water by Ion Exchange. Richmond,
California, Sea-Water Conversion Laboratory, Report No. 63-2,
February. (also Ind. Eng. Chem., Proc. Des. Dev., 3, 3 (1964),
280-287).

Lantz, R. B. 1971. "Quantative Evaluation of Numerical Diffusion
(Truncation Error)." Soc. Pet. Eng. J., September, 315-320.

Larson, R. G. 1982. "Controlling Numerical Dispersion By Variably
Timed Flux Updating in One Dimension." Soc. Pet. Eng. J., June,
399-408.

Laumbach, D. D. 1975. "A High-Accuracy Finite-Difference Technique for
Treating the Cnvection-Diffusion Equation." Soc. Pet. Eng. J.,
December, 517-531.

Martin, A. J. P., R. L. M. Synge. 1941. "A New Form of Chromatogram
Employing Two Liquid Phases." Biochem. J., 35, 1358-1368.

Mayer, S. W., E. R. Tompkins. 1947. "Ion Exchange as a Separations
Method. IV. A Theoretical Analysis of the Column Separations
Process." J. Amer. Chem. Soc., 69, 2866-2874.

Pandya, P. J., G. Klein, T. Vermeulen. 1965. Saline Water Softening by
Fixed-Bed Ion Exchange. Equilbrium Stage Computation Method for
Multicomponent Systems. Richmond, California, Sea Water Conversion
Laboratory, Report No. 65-1, June.

Peaceman, D. W., H. H. Rachford, Jr. 1955. "The Numerical Solution of Parabolic and Elliptic Differential Equations." $\underline{J}$. $\underline{Soc}$. $\underline{Ind}$. $\underline{Appl}$. $\underline{Math}$., 3, 1, 28-41.

Peaceman, D. W., H. H. Rachford, Jr. 1962. "Numerical Calculation of Multidimensional Miscible Displacement." $\underline{Soc}$. $\underline{Pet}$. $\underline{Eng}$. $\underline{J}$., December, 327-339.

Price, H. S., J. C. Cavendish, R. S. Varga. 1968. "Numerical Methods of Higher-Order Accuracy for Diffusion-Convection Equations." $\underline{Soc}$. $\underline{Pet}$. $\underline{Eng}$. $\underline{J}$., September, 293-303.

Price, H. S., R. S. Varga, J. E. Warren. 1966. "Application of Oscillation Matrices to Diffusion-Convection Equations." $\underline{J}$. $\underline{Math}$. $\underline{Phys}$., 45, 301-311.

Stone, H. L., P. L. T. Brian. 1963. "Numerical Solution of Convective Transport Problems." $\underline{AIChE}$ $\underline{J}$., 9, 5, 681-688.

Vassiliou, B., J. S. Dranoff. 1962. "The Kinetics of Ion Exclusion." $\underline{AIChE}$ $\underline{J}$., 8, 2, 248-252.

VonNeumann, J., R. D. Richtmeyer. 1950. "A Method for the Numerical Calculation of Hydrodynamic Shocks." $\underline{J}$. $\underline{Appl}$. $\underline{Phys}$. 21, 232-237.

Walter, J. E. 1945. "Multiple Adsorption From Solutions." $\underline{J}$. $\underline{Chem}$. $\underline{Phys}$., 13, 6, 229-234.

Weiss, J. 1943. "On the Theory of Chromatography." $\underline{J}$. $\underline{Chem}$. $\underline{Soc}$.,$\underline{London}$, 297-303.

Wilson, J. N. 1940. "A Theory of Chromatography." $\underline{J}$. $\underline{Amer}$. $\underline{Chem}$. $\underline{Soc}$., 62, 1583-1591.

APPENDIX A

LISTING OF COMPUTER PROGRAM

```
C****************************************************************
C
C        THIS PROGRAM APPROXIMATES THE SOLUTION TO THE
C        ONE-DIMENSIONAL, TRANSIENT CONVECTION-DISPERSION
C        EQUATION APPLIED TO AN EQUILIBRIUM ION EXCHANGE PROCESS.
C
C****************************************************************
C        *NOMENCLATURE
C
C        A,B,C,D: Overall coefficients of finite difference
C         equation for use in recursive solution of tridiagonal
C         matrix.
C        AEMPTY: Total cross-sectional area of column.
C        AFNM1: Absolute value of FNM1.
C        AX,ALP: Accumulation coefficients in finite difference
C         equation.
C        BEDDIA: Resin bed diameter.
C        BET: Dispersive coefficient in finite-difference equation.
C        BETA,GAMMA: Factors in matrix solution routine.
C        CON: Array of ionic concentrations.
C        CPRIME: Inlet solution concentration.
C        CSMAX: Maximum attainable resin concentration.
C        CZERO: Initial resin concentration.
C        DEL: Convective coefficient in finite-difference equation.
C        DELTAM: Absolute value of difference between actual mass
C         input and numerically calculated input, at time T.
C        DELTAP: Pressure drop over entire column.
C        DELTAT: Temporal increment.
C        DELTAV: Volume increment.
C        DELTAZ: Spatial increment.
C        DMBAR: Averaged value of material balance closure.
C        DMBARO: Material balance closure over entire simulation.
C        DP: Resin particle diameter.
C        DSUBZ: Hydrodynamic dispersion coefficient.
C        DZNUM: Numerical dispersion coefficient.
C        D1,D2,D3: Components of coefficient D.
C        FK: Equilibrium constant in isotherm equation.
C        FN: Exponent in isotherm equation.
C        IF,L: First and last increment subscripts in matrix solution.
C        ISO: Isotherm selection number.
C        KI: Input device number.
C        KO: Output device number.
C        KT,J: Time loop counters.
C        L,M,N: Increment numbers of Z1Q,Z1H,Z3Q respectively.
C        NEWDAT: Interactive data-change parameter.
C        NEWSEL: Interactive data-change parameter.
C        N2SEL: Interactive data-change parameter.
C        NEXT: End-of-simulation operation selection parameter.
C        NINC: Number of spatial increments.
C        NP1: Number of last spatial increment.
C        PIN: Inlet pressure.
C        POROS: Resin bed porosity.
C        POUT: Outlet pressure.
C        REP: Particle Reynolds number.
```

```
C      RHOL: Solution density.
C      T: Time.
C      TEST: Interstitial flow regime determination factor.
C      TITLE: Optional simulation output title.
C      TMAX: Total simulation time.
C      TOUT: Desired time increment for output.
C      V: Solution array from matrix solution routine.
C      VEL: Average interstitial solution velocity.
C      VISC: Solution viscosity.
C      VOLFLO: Solution volumetric flow rate.
C      WS: Superficial velocity..
C      XINCL,XL: Height of resin bed.
C      Z1Q,Z1H,Z3Q: One fourth, one half, and three fourths
C       of XL, respectively.
C
C      **SUBROUTINES
C       *BEDPAR
C         Arguments: AEMPTY,BEDDIA,DELTAT,DELTAZ,DP,DSUBZ,IT,KI,KO,
C                    NEXT,NINC,POROS,RHOL,TOUT,VEL,VISC,VOLFLO
C       *DATA
C         Arguments: BEDDIA,CPRIME,CZERO,KI,KO,NEXT,NINC,PIN,POROS,
C                    RHOL,TMAX,VISC,VOLFLO,XL
C       *DELP
C         Arguments: BEDDIA,DELTAP,DP,KO,POROS,RHOL,TEST,VISC,VOLFLO,
C                    XINCL
C       *DETISO
C         Arguments:  CSMAX,FK,FN,ISO,KI,KO
C       *TRIDAG
C         Arguments: A,B,BETA,C,D,GAMMA,IF,L,NP1,VC
C*******************************************************************
C
      IMPLICIT REAL*8(A-H,O-Z)
      DIMENSION CON(501),A(501),B(501),C(501),D(501),AX(501),
     1 BETA(501),GAMMA(501),ALP(501),IO(12)
      KO=6
      KI=5
C
C  INITIALIZE TIME AND TIME COUNTERS.
   60 T=0.
      KT=0
      J=1
C
C  INPUT SYSTEM DATA.
      CALL DATA(NINC,DP,RHOL,VOLFLO,XL,BEDDIA,POROS,VISC,
     1 PIN,CZERO,CPRIME,TMAX,KO,KI,NEXT,NEWDAT,NEWSEL)
C
C  SPECIFY ISOTHERM TYPE.
      IF(NEXT.EQ.3)WRITE(KO,8)
      IF(NEXT.EQ.3)READ(KI,1)NEWISO
      IF(NEXT.EQ.3.AND.NEWISO.EQ.O)GO TO 15
      CALL DETISO(KO,KI,FK,FN,CSMAX,ISO)
   15 CONTINUE
C
C  DEFINE SPATIAL INCREMENT, DELTAZ(FT).
```

```
      DELTAZ=XL/FLOAT(NINC)
C
C COMPUTE INTERSTITIAL VELOCITY AND DISPERSION COEFFICIENT
C   IN SUBROUTINE BEDPAR.
      CALL BEDPAR(DELTAT,AEMPTY,DELTAZ,NINC,DP,RHOL,IT,VOLFLO,
     1 BEDDIA,POROS,VISC,VZ,DZ,KO,KI,NEXT)
C
C CALCULATE VOLUME INCREMENT, DELTAV
      DELTAV=AEMPTY*POROS*DELTAZ
      NP1=NINC+1
C
C INITIALIZE CONCENTRATIONS AT ALL SPATIAL NODES.
      DO 10 I=1,NP1
   10 CON(I)=CZERO
C
      WRITE(KO,2)VZ,DZ
C
C DETERMINE DELTAP FOR ENTIRE COLUMN IN SUBROUTINE DELP.
      CALL DELP(DP,RHOL,VOLFLO,BEDDIA,POROS,XL,VISC,TEST,DELTAP,KO)
C CORRECT UNITS OF DELTAP.
      DELTAP=DELTAP/144.
      WRITE(KO,3)DELTAP
C
C CALCULATE OUTLET PRESSURE.
      POUT=PIN-DELTAP
      WRITE(KO,4)POUT
C
C CALCULATE FRACTIONAL COLUMN LENGTHS, Z1Q, Z1H, AND Z3Q.
      Z1Q=.25*XL
      Z1H=.5*XL
      Z3Q=.75*XL
      WRITE(KO,5)Z1Q,Z1H,Z3Q
      L=INT(Z1Q/DELTAZ)
      M=INT(Z1H/DELTAZ)
      N=INT(Z3Q/DELTAZ)
C
C PRINT INITIAL BED CONCENTRATIONS AT TOP, 1/4-1/2-3/4 COLUMN
C   LENGTH, AND BOTTOM OF COLUMN.
      WRITE(KO,6)T,CON(1),CON(L),CON(M),CON(N),CON(NP1)
C
C DEFINE DISPERSIVE AND CONVECTIVE TERMS, BET AND DEL,
C   RESPECTIVELY, IN DIFFERENCE EQUATIONS.
      BET=DZ/2./DELTAZ/DELTAZ
      DEL=VZ/4./DELTAZ
C
C CALCULATE ACCUMULATION TERM, AX, FOR USE IN DIFFERENCE EQUATIONS,
C   BASED ON ISOTHERM TYPE.
   70 DO 20 I=2,NP1
      IF(ISO.EQ.1)AX(I)=(1.+FK*(1.-POROS)/POROS)
      IF(ISO.EQ.2)
     1 AX(I)=(1.+FK*CSMAX*(1.-POROS)/POROS)/((1.
     2 +FK*CON(I))**2)
      FNM1=FN-1.
      AFNM1=ABS(FNM1)
```

```fortran
      IF(ISO.EQ.3.AND.FNM1.GE.0..AND.CON(I).NE.0.)
     1 AX(I)=(1.+FN*FK*(CON(I)**FNM1)*(1.-POROS)/POROS)
      IF(ISO.EQ.3.AND.FNM1.LT.0..AND.CON(I).NE.0.)
     1 AX(I)=(1.+(1.-POROS)*FN*FK*(1./CON(I)**AFNM1)/POROS)
      IF(ISO.EQ.3.AND.CON(I).EQ.0.)
     1 AX(I)=1.
   20 CONTINUE
C
C SET UP MATRICES OF FINITE-DIFFERENCE COEFFICIENTS FOR USE IN
C   SOLUTION OF THE TRIDIAGONAL MATRIX.
      DO 30 I=2,NP1
      ALP(I)=AX(I)/DELTAT
      A(I)=-BET-DEL
      B(I)=ALP(I)+2.*BET
      C(I)=-BET+DEL
      D1=BET+DEL
      D2=ALP(I)-2.*BET
      D3=BET-DEL
   30 D(I)=D1*CON(I-1)+D2*CON(I)+D3*CON(I+1)
      D(2)=(BET+DEL)*CPRIME+D(2)
      B(NP1)=ALP(NP1)+BET+DEL
      D(NP1)=(D2+D3)*CON(NP1)+D1*CON(NINC)
C
C CALCULATE NEW CONCENTRATIONS AT T=T+DELTAT; CONCENTRATION AT
C  TOP OF COLUMN IS CONSTANT(CPRIME) BY BOUNDARY CONDITION.
      CON(1)=CPRIME
      CALL TRIDAG(NP1,2,NP1,A,B,C,D,BETA,GAMMA,CON)
C
C CHECK MATERIAL BALANCE
      IF(T.EQ.0.)GO TO 80
      TMASS1=VOLFLO*CPRIME*T
      TMASS3=0.
      DO 90 I=1,NP1
      TMASS2=CON(I)*DELTAV
   90 TMASS3=TMASS3+TMASS2
      DELTAM=ABS(TMASS1-TMASS2)
      DMBAR=DMBAR+DELTAM
   80 T=T+DELTAT
      IF((J/IT)*IT.NE.J)GO TO 40
C
C PRINT UPDATED CONCENTRATIONS AT TOP, 1/4-1/2-3/4 COLUMN LENGTH,
C  AND BOTTOM OF COLUMN.
      WRITE(KO,6)T,CON(1),CON(L),CON(M),CON(N),CON(NP1)
C
C INCREMENT TIME COUNTERS AND TIME
   40 J=J+1
      KT=KT+1
      T=DELTAT*FLOAT(KT)
      DMBARO=DMBAR/FLOAT(KT)
      IF(T.EQ.TMAX)WRITE(KO,9)DMBARO
      IF(T.LT.TMAX)GO TO 70
      WRITE(KO,7)
      READ(KI,1)NEXT
    1 FORMAT(I5)
```

```
   GO TO (50,60,60),NEXT
2 FORMAT(1X,'AVERAGE INTERSTITIAL VELOCITY=',E15.5,1X,'FT/SEC'
 1 ,//,1X,'DISPERSION COEFFICIENT(HYDRODYNAMIC - NUMERICAL)='
 2 ,E15.5,1X,'FT2/SEC',/)
3 FORMAT(1X,'DELTAP=',E15.5,1X,'PSI',/)
4 FORMAT(1X,'OUTLET PRESSURE=',E15.5,1X,'PSI',/)
5 FORMAT(//,1X,'CONCENTRATION AS FUNCTION OF TIME AND DISTANCE',//,
 1 2X,'TIME(SEC)',5X,'TOP',6X,F7.2,1X,'FT',4X,F7.2,1X,'FT',3X,F7.2,
 2 1X,'FT',6X,'BOTTOM',/)
6 FORMAT(3X,F7.2,5E13.5)
7 FORMAT(1X,'SIMULATION COMPLETE--WHAT NEXT?',//,1X,'1-STOP',
 1 /,1X,'2-NEW PROBLEM',/,1X,'3-ALTER PARAMETERS OF PREVIOUS
 2 PROBLEM',//,1X,'ENTER SELECTION NUMBER',/)
8 FORMAT(1X,'WOULD YOU LIKE TO CHANGE ISOTHERM DATA?'
 1 ,/,5X,'1-YES',5X,'0-NO',/)
9 FORMAT(/,1X,'AVERAGE ERROR IN TOTAL MATERIAL BALANCE =',E15.5,
 1 1X,'LB/FT3',//)
50 END
```

```fortran
      SUBROUTINE BEDPAR(DELTAT,AEMPTY,DELTAZ,NINC,DP,RHOL,
     1 IT,VOLFLO,BEDDIA,POROS,VISC,VEL,DSUBZ,KO,KI,NEXT)
C*******************************************
C    SUBROUTINE TO CALCULATE BED PARAMETERS
C*******************************************
      IMPLICIT REAL*8(A-H,O-Z)
      DIMENSION IO(12)
      DATA IO/100,1000,10000,100000,10,100,1000,10000,1,10,100,1000/
C
C   CALCULATE PARTICLE REYNOLDS NUMBER
      AEMPTY=3.1416*(BEDDIA**2)/4.
      VEL=VOLFLO/AEMPTY/POROS
      IF(NEXT.EQ.3)WRITE(KO,4)
      IF(NEXT.EQ.3)READ(KI,2)NEWTEM
      IF(NEXT.EQ.3.AND.NEWTEM.EQ.O)GO TO 6
      WRITE(KO,1)
      READ(KI,2)IT
      IF(IT.EQ.1)DELTAT=.01
      IF(IT.EQ.2)DELTAT=.1
      IF(IT.EQ.3)DELTAT=1.
      WRITE(KO,3)
      READ(KI,2)IOUT
      IT=IO(IOUT)
    6 REP=DP*RHOL*VEL/VISC
C
C   CALCULATE DISPERSION COEFFICIENT BASED ON HARLEMAN(1963)
C   INCLUDE NUMERICAL DISPERSION COEFFICIENT
      DSUBZ=.66*VISC*(REP**1.2)/RHOL
      DZNUM=.5*VEL*VEL*DELTAT/POROS
      DSUBZ=DSUBZ+DZNUM
C
    1 FORMAT(1X,'ENTER TIME INCREMENT, SEC',/,2X,'1-.01',
     1 4X,'2-.1',4X,'3-1.0',/)
    2 FORMAT(I4)
    3 FORMAT(1X,'HOW OFTEN WOULD YOU LIKE TO READ THE CONCENT
     1RATION PROFILE?',/,1X,'ENTER SELECTION NUMBER FROM BELOW'
     2 ,//,2X,'DELTAT=.01 SEC',5X,'DELTAT=.1 SEC',5X,'DELTAT=
     31 SEC',/,3X,'1-',3X,'1 SEC',9X,'5-',3X,'1 SEC',9X,'9-',3X
     4,'1 SEC',/,3X,'2-',2X,'10 SEC',9X,'6-',2X,'10 SEC',8X,'10-
     5',2X,'10 SEC',/,3X,'3-',1X,'100 SEC',9X,'7-',1X,'100 SEC',
     6 8X,'11-',1X,'100 SEC',/,3X,'4-1000 SEC',9X,'8-1000 SEC'
     7 ,8X,'12-1000 SEC',/)
    4 FORMAT(1X,'WOULD YOU LIKE TO CHANGE TIME INCREMENT
     1 OR OUTPUT INTERVAL?',/,5X,'1-YES',5X,'0-NO',/)
      RETURN
      END
```

```
      SUBROUTINE DATA (NINC,DP,RHOL,VOLFLO,XL,BEDDIA,POROS,
     1 VISC,PIN,CZERO,CPRIME,TMAX,KO,KI,NEXT,NEWDAT,NEWSEL)
C***************************
C  SUBROUTINE TO INPUT DATA
C***************************.
      IMPLICIT REAL*8(A-H,O-Z)
      DIMENSION TITLE(15)
      IF(NEXT.EQ.3)NEWDAT=1
      IF(NEXT.EQ.3)GO TO 55
   40 WRITE(KO,2)
      READ(KI,3)(TITLE(I),I=1,15)
      IF(NEWDAT.EQ.1)GO TO 53
      WRITE(KO,1)
   41 WRITE(KO,4)
      READ(KI,5)XL
      IF(NEWDAT.EQ.1)GO TO 53
   42 WRITE(KO,6)
      READ(KI,5)BEDDIA
      IF(NEWDAT.EQ.1)GO TO 53
   43 WRITE(KO,20)
      READ(KI,21)NINC
      IF(NEWDAT.EQ.1)GO TO 53
   44 WRITE(KO,7)
      READ(KI,5)VOLFLO
      IF(NEWDAT.EQ.1)GO TO 53
   45 WRITE(KO,8)
      READ(KI,5)RHOL
      IF(NEWDAT.EQ.1)GO TO 53
   46 WRITE(KO,9)
      READ(KI,5)VISC
      IF(NEWDAT.EQ.1)GO TO 53
   47 WRITE(KO,10)
      READ(KI,5)DP
      IF(NEWDAT.EQ.1)GO TO 53
   48 WRITE(KO,11)
      READ(KI,5)POROS
      IF(NEWDAT.EQ.1)GO TO 53
   49 WRITE(KO,12)
      READ(KI,5)PIN
      IF(NEWDAT.EQ.1)GO TO 53
   50 WRITE(KO,13)
      READ(KI,5)CZERO
      IF(NEWDAT.EQ.1)GO TO 53
   51 WRITE(KO,14)
      READ(KI,5)CPRIME
      IF(NEWDAT.EQ.1)GO TO 53
   52 WRITE(KO,24)
      READ(KI,5)TMAX
      IF(NEWDAT.EQ.1)GO TO 53
C  PRINT SUMMARY OF INPUT DATA
      WRITE(KO,15)(TITLE(I),I=1,15),XL,BEDDIA,NINC,VOLFLO,RHOL,
     1VISC,DP,POROS,PIN,CZERO,CPRIME
      WRITE(KO,23)
      WRITE(KO,16)
```

```
      READ(KI,21)NEWDAT
   55 IF(NEWDAT.EQ.1)WRITE(KO,19)
      IF(NEWDAT.EQ.0)GO TO 22
   54 READ(KI,21)NEWSEL
      GO TO (40,41,42,43,44,45,46,47,48,49,50,51,52),NEWSEL
   53 WRITE(KO,17)
      READ(KI,21)N2SEL
      IF(N2SEL.EQ.1)WRITE(KO,18)
      IF(N2SEL.EQ.1)GO TO 54
      IF(NEWDAT.EQ.1.AND.N2SEL.EQ.0)WRITE(KO,15)
    1 (TITLE(I),I=1,15),XL,BEDDIA,NINC,VOLFLO,RHOL,VISC,
    2 DP,POROS,PIN,CZERO,CPRIME
      GO TO 22
C
C  INTERACTIVE FORMATS
    1 FORMAT(1X,'------INPUT DATA------',//)
    2 FORMAT(1X,'ENTER TITLE, 60 CHARACTERS MAXIMUM',/)
    3 FORMAT(15A4)
    4 FORMAT(1X,'ENTER COLUMN HEIGHT, FT',/)
    5 FORMAT(F15.0)
    6 FORMAT(1X,'ENTER COLUMN DIAMETER, FT',/)
    7 FORMAT(1X,'ENTER SOLUTION VOLUMETRIC FLOW RATE, FT3/SEC',/)
    8 FORMAT(1X,'ENTER SOLUTION DENSITY, LB/FT3',/)
    9 FORMAT(1X,'ENTER SOLUTION VISCOSITY, LB/FT/SEC',/)
   10 FORMAT(1X,'ENTER RESIN PARTICLE DIAMETER, FT',/)
   11 FORMAT(1X,'ENTER RESIN POROSITY',/)
   12 FORMAT(1X,'ENTER INLET PRESSURE, PSI',/)
   13 FORMAT(1X,'ENTER INITIAL RESIN CONCENTRATION, LB/FT3',/)
   14 FORMAT(1X,'ENTER INLET SOLUTION CONCENTRATION, LB/FT3',/)
   15 FORMAT(1X,52('*')/,3X,'DATA SUMMARY FOR:',
    1 1X,15A4,/,4X,'COLUMN HEIGHT(FT):',31X,E10.4,1X,/,
    2 4X,'COLUMN DIAMETER(FT):',29X,E10.4,1X,/,4X,'NUMBER OF ',
    3 'SPATIAL INCREMENTS:',22X,I4,/,4X,'SOLUTION VOLUMETRIC ',
    4 'FLOW RATE(FT3/SEC):',10X,E10.4,1X,/,4X,
    5 'SOLUTION DENSITY(LB/FT3):'
    6 ,24X,E10.4,1X,/,4X,'SOLUTION VISCOSITY(LB/FT/SEC):',19X,
    7 E10.4,1X,/,4X,'RESIN PARTICLE DIAMETER(FT):',
    8 21X,E10.4,1X,/,4X,'RESIN POROSITY:',34X,E10.4,/,4X,
    9 'INLET PRESSURE(PSI):',29X,E10.4,1X,/,4X,'INITIAL BED ',
    A 'CONCENTRATION(LB/FT3):',15X,E10.4,1X,/,4X,'INLET ',
    B 'SOLUTION CONCENTRATION(LB/FT3):',12X,E10.4,/
    C ,1X,52('*')/)
   16 FORMAT(1X,'WOULD YOU LIKE TO CHANGE ANY OF THESE VALUES?'/
    1 5X,'1-YES',5X,'0-NO',/)
   17 FORMAT(1X,'WOULD YOU LIKE TO CHANGE ANY OTHER VALUES?',/
    1 5X,'1-YES',5X,'0-NO',/)
   18 FORMAT(1X,'ENTER NUMBER OF QUANTITY TO BE CHANGED',/)
   19 FORMAT(1X,'DATA CHANGE MENU',/1X,31('*')
    1 ,/,2X,'1-TITLE',/,2X,'2-COLUMN HEIGHT',/,2X,'3-COLUMN DIAMETER'
    2 ,/,2X,'4-NUMBER OF INCREMENTS',/,2X,'5-VOLUMETRIC FLOW ',
    3 'RATE',/,2X,'6-SOLUTION DENSITY',/,2X,'7-SOLUTION VISCOSITY'
    4 ,/,2X,'8-RESIN PARTICLE DIAMETER',/,2X,'9-RESIN POROSITY',/,
    5 1X,'10-INLET PRESSURE',/,1X,'11-INITIAL RESIN CONCENTRATION'
    6 ,/,1X,'12-INLET SOLUTION CONCENTRATION',/,1X,'13-MAXIMUM ',
```

```
   7 'SIMULATION TIME',/,1X,31('*')
   8 //,1X,'ENTER NUMBER OF QUANTITY TO BE CHANGED',/)
  20 FORMAT(1X,'ENTER NUMBER OF SPATIAL INCREMENTS,500 MAX',/)
  21 FORMAT(I4)
  23 FORMAT(1X,52('*')/)
  24 FORMAT(1X,'ENTER MAXIMUM SIMULATION TIME, SEC',/)
  22 RETURN
     END
```

```fortran
      SUBROUTINE DELP(DP,RHOL,VOLFLO,BEDDIA,POROS,XINCL,VISC,TEST,
     1 DELTAP,KO)
C********************************************
C  SUBROUTINE FOR PRESSURE DROP CALCULATION
C********************************************
      IMPLICIT REAL*8(A-H,O-Z)
C
C  CALCULATE SUPERFICIAL VELOCITY, WS(FT/SEC)
      AEMPTY=3.1416*(BEDDIA**2)/4.
      WS=VOLFLO/AEMPTY
C
C  DETERMINE FLOW REGIME
      TEST=DP*RHOL*WS/VISC/(1.-POROS)
      IF(TEST.GT.1000.)GO TO 5
      IF(TEST.GT.10..AND.TEST.LT.1000.)GO TO 6
C
C  PRESSURE DROP FOR LAMINAR FLOW(BLAKE-KOZENY EQUATION)
      DELTAP=WS*XINCL*150.*VISC*((1.-POROS)**2)/(DP**2)/(POROS**3)/32.2
      WRITE(KO,1)
      GO TO 4
C
C  PRESSURE DROP FOR TURBULENT FLOW(BURKE-PLUMMER EQUATION)
    5 DELTAP=1.75*XINCL*RHOL*(WS**2)*(1.-POROS)/DP/(POROS**3)/32.2
      WRITE(KO,2)
      GO TO 4
C
C  PRESSURE DROP FOR TRANSITION FLOW(ERGUN EQUATION)
    6 DELTAP=WS*XINCL*150.*VISC*((1.-POROS)**2)/(DP**2)/(POROS**3)/32.2
     1+1.75*XINCL*RHOL*(W**2)*(1.-POROS)/DP/(POROS**3)/32.2
      WRITE(KO,3)
    4 CONTINUE
C
    1 FORMAT(1X,'LAMINAR FLOW REGIME',//)
    2 FORMAT(1X,'TURBULENT FLOW REGIME',//)
    3 FORMAT(1X,'TRANSITION FLOW REGIME',//)
      RETURN
      END
```

```fortran
      SUBROUTINE DETISO(KO,KI,FK,FN,CSMAX,ISO)
C*************************************
C  SUBROUTINE TO SPECIFY ISOTHERM TYPE
C*************************************
      IMPLICIT REAL*8(A-H,O-Z)
      WRITE(KO,1)
      READ(KI,2)ISO
      IF(ISO.NE.1)GO TO 9
      WRITE(KO,3)
      READ(KI,5)FK
      FN=0.
      CSMAX=0.
      GO TO 11
    9 IF(ISO.NE.2)GO TO 10
      WRITE(KO,4)
      READ(KI,5)FK
      WRITE(KO,6)
      READ(KI,5)CSMAX
      FN=0.
      GO TO 11
   10 IF(ISO.EQ.3)WRITE(KO,7)
      READ(KI,5)FK
      WRITE(KO,8)
      READ(KI,5)FN
      CSMAX=0.
   11 CONTINUE
    1 FORMAT(1X,'ENTER ISOTHERM TYPE',//,1X,'1-LINEAR',10X,'2
     1-LANGMUIR',10X,'3-FREUNDLICH',//)
    2 FORMAT(I1)
    3 FORMAT(1X,'LINEAR ISOTHERM',//,1X,'ENTER EQUILIBRIUM CON
     1STANT',//)
    4 FORMAT(1X,'LANGMUIR ISOTHERM',//,1X,'ENTER EQUILIBRIUM CONSTANT'
     1,//)
    5 FORMAT(F15.5)
    6 FORMAT(1X,'ENTER MAXIMUM RESIN CONCENTRATION',//)
    7 FORMAT(1X,'FREUNDLICH ISOTHERM',//,1X,'ENTER EQUILIBRIUM
     1 CONSTANT',/)
    8 FORMAT(1X,'ENTER EXPONENT FOR SOLUTION CONCENTRATION',/)
      RETURN
      END
```

```fortran
      SUBROUTINE TRIDAG(NP1,IF,L,A,B,C,D,BETA,GAMMA,V)
C*****************************************
C  SUBROUTINE TO SOLVE TRIDIAGONAL SYSTEM
C*****************************************
      IMPLICIT REAL*8(A-H,O-Z)
      DIMENSION A(NP1),B(NP1),C(NP1),D(NP1),V(NP1),BETA(NP1),
     1 GAMMA(NP1)
      BETA(IF)=B(IF)
      GAMMA(IF)=D(IF)/BETA(IF)
      IFP1=IF+1
      DO 1 I=IFP1,L
      BETA(I)=B(I)-A(I)*C(I-1)/BETA(I-1)
    1 GAMMA(I)=(D(I)-A(I)*GAMMA(I-1))/BETA(I)
      V(L)=GAMMA(L)
      LAST=L-IF
      DO 2 K=1,LAST
      I=L-K
    2 V(I)=GAMMA(I)-C(I)*V(I+1)/BETA(I)
      RETURN
      END
```

APPENDIX B

SAMPLE INPUT DIALOG/OUTPUT FORMAT

```
ENTER TITLE, 60 CHARACTERS MAXIMUM

SAMPLE INPUT DIALOG/OUTPUT FORMAT
------INPUT DATA------


ENTER COLUMN HEIGHT, FT

2.297
ENTER COLUMN DIAMETER, FT

.0446
ENTER NUMBER OF SPATIAL INCREMENTS,500 MAX

100
ENTER SOLUTION VOLUMETRIC FLOW RATE, FT3/SEC

5.916E-06
ENTER SOLUTION DENSITY, LB/FT3

62.94
ENTER SOLUTION VISCOSITY, LB/FT/SEC

.0008
ENTER RESIN PARTICLE DIAMETER, FT

.0017
ENTER RESIN POROSITY

.4
ENTER INLET PRESSURE, PSI

20
ENTER INITIAL RESIN CONCENTRATION, LB/FT3

0
ENTER INLET SOLUTION CONCENTRATION, LB/FT3

2.56
ENTER MAXIMUM SIMULATION TIME, SEC

100
**********************************************************
  DATA SUMMARY FOR: SAMPLE INPUT DIALOG/OUTPUT FORMAT
   COLUMN HEIGHT(FT):                             0.2297E+01
   COLUMN DIAMETER(FT):                           0.4460E-01
   NUMBER OF SPATIAL INCREMENTS:                        100
   SOLUTION VOLUMETRIC FLOW RATE(FT3/SEC):        0.5916E-05
   SOLUTION DENSITY(LB/FT3):                      0.6294E+02
   SOLUTION VISCOSITY(LB/FT/SEC):                 0.8000E-03
   RESIN PARTICLE DIAMETER(FT):                   0.1700E-02
   RESIN POROSITY:                                0.4000E+00
   INLET PRESSURE(PSI):                           0.2000E+02
   INITIAL BED CONCENTRATION(LB/FT3):             0.0000E+00
   INLET SOLUTION CONCENTRATION(LB/FT3):          0.2560E+01
**********************************************************
```

```
WOULD YOU LIKE TO CHANGE ANY OF THESE VALUES?
     1-YES        0-NO


1
DATA CHANGE MENU
*******************************
 1-TITLE
 2-COLUMN HEIGHT
 3-COLUMN DIAMETER
 4-NUMBER OF INCREMENTS
 5-VOLUMETRIC FLOW RATE
 6-SOLUTION DENSITY
 7-SOLUTION VISCOSITY
 8-RESIN PARTICLE DIAMETER
 9-RESIN POROSITY
10-INLET PRESSURE
11-INITIAL RESIN CONCENTRATION
12-INLET SOLUTION CONCENTRATION
13-MAXIMUM SIMULATION TIME
*******************************


ENTER NUMBER OF QUANTITY TO BE CHANGED


1
ENTER TITLE, 60 CHARACTERS MAXIMUM

SAME TEST- SAMPLE DIALOG/FORMAT
WOULD YOU LIKE TO CHANGE ANY OTHER VALUES?
     1-YES        0-NO


0
*****************************************************
  DATA SUMMARY FOR: SAME TEST- SAMPLE DIALOG/FORMAT
   COLUMN HEIGHT(FT):                          0.2297E+01
   COLUMN DIAMETER(FT):                        0.4460E-01
   NUMBER OF SPATIAL INCREMENTS:                  100
   SOLUTION VOLUMETRIC FLOW RATE(FT3/SEC):     0.5916E-05
   SOLUTION DENSITY(LB/FT3):                   0.6294E+02
   SOLUTION VISCOSITY(LB/FT/SEC):              0.8000E-03
   RESIN PARTICLE DIAMETER(FT):                0.1700E-02
   RESIN POROSITY:                             0.4000E+00
   INLET PRESSURE(PSI):                        0.2000E+02
   INITIAL BED CONCENTRATION(LB/FT3):          0.0000E+00
   INLET SOLUTION CONCENTRATION(LB/FT3):       0.2560E+01
*****************************************************
```

```
ENTER ISOTHERM TYPE

1-LINEAR            2-LANGMUIR            3-FREUNDLICH


1
LINEAR ISOTHERM

ENTER EQUILIBRIUM CONSTANT


.58
ENTER TIME INCREMENT, SEC
 1-.01    2-.1    3-1.0

3
HOW OFTEN WOULD YOU LIKE TO READ THE CONCENTRATION PROFILE?
ENTER SELECTION NUMBER FROM BELOW

DELTAT=.01 SEC     DELTAT=.1 SEC     DELTAT=1 SEC
  1-   1 SEC        5-   1 SEC        9-   1 SEC
  2-  10 SEC        6-  10 SEC       10-  10 SEC
  3- 100 SEC        7- 100 SEC       11- 100 SEC
  4-1000 SEC        8-1000 SEC       12-1000 SEC


10
```

AVERAGE INTERSTITIAL VELOCITY=   0.94669E-02 FT/SEC

DISPERSION COEFFICIENT(HYDRODYNAMIC - NUMERICAL)=   0.12316E-03 FT2/SEC

LAMINAR FLOW REGIME

DELTAP=   0.43814E+00 PSI

OUTLET PRESSURE=   0.19562E+02 PSI

CONCENTRATION AS FUNCTION OF TIME AND DISTANCE

TIME(SEC)	TOP	0.57 FT	1.15 FT	1.72 FT	BOTTOM
0.00	0.00000E+00	0.00000E+00	0.00000E+00	0.00000E+00	0.00000E+00
10.00	0.25600E+01	0.11012E-13	0.18859E-35	0.00000E+00	0.00000E+00
20.00	0.25600E+01	0.97093E-09	0.14194E-27	0.00000E+00	0.00000E+00
30.00	0.25600E+01	0.91213E-06	0.56319E-22	0.00000E+00	0.00000E+00
40.00	0.25600E+01	0.81733E-04	0.95578E-18	0.15078E-35	0.00000E+00
50.00	0.25600E+01	0.18132E-02	0.19264E-14	0.99811E-31	0.00000E+00
60.00	0.25600E+01	0.16279E-01	0.84292E-12	0.10890E-26	0.00000E+00
70.00	0.25600E+01	0.78479E-01	0.11811E-09	0.29239E-23	0.00000E+00
80.00	0.25600E+01	0.24250E+00	0.68987E-08	0.25597E-20	0.28804E-36
90.00	0.25600E+01	0.54084E+00	0.20234E-06	0.89962E-18	0.99874E-33
100.00	0.25600E+01	0.94719E+00	0.34122E-05	0.14864E-15	0.13923E-29

AVERAGE ERROR IN TOTAL MATERIAL BALANCE =   0.74968E-03 LB/FT3

SIMULATION COMPLETE--WHAT NEXT?

1-STOP
2-NEW PROBLEM
3-ALTER PARAMETERS OF PREVIOUS PROBLEM

ENTER SELECTION NUMBER

APPENDIX C

EXPERIMENTAL DATA FROM THE LITERATURE

Linear Isotherm System

Vassiliou and Dranoff (1962) reported experiments on the exclusion of glycerol from aqueous solutions using a small fixed-bed columns of a hydrogen form ion exchange resin. The reported data is summarized below in appropriate units for use in the computer program of Appendix A.

Column Characteristics: $L = 2.297$ ft.
$D_c = 0.0446$ ft.

Solution Characteristics: $\dot{V} = 5.916\text{e-}06$ ft^3/sec
$\rho = 62.94$ lb/ft^3
$\mu = 0.0008$ lb/ft/sec
$C_{in} = 2.56$ lb/ft^3

Resin Characteristics: $D_p = 0.0017$ ft.

$\varepsilon = 0.4$
$F_k = 0.58$

Breakthrough Data:

t, sec	C/Co
257	0.030
269	0.045
292	0.100
306	0.160
333	0.300
365	0.470
393	0.600
424	0.701
483	0.850
543	0.930
603	0.980
660	1.000

Freundlich Isotherm System

Erickson (1979) reported experiments performed on the ethylenediamine dihydrochloride and ammonium chloride system. The ion exchange equilibrium was described by a Freundlich isotherm for

favorable and unfavorable exchange. The reported data are summarized below for use in the computer program of Appendix A.

Favorable Exchange

Column Characteristics: L = 1.732 ft.

D_c = 0.1306 ft.

Solution Characteristics: $\dot{V}$ = 0.812e-03 ft^3/sec

ρ = 62.22 lb/ft^3

μ = 0.0006 lb/ft/sec

C_{in} = 1.985 lb/ft^3

Resin Characteristics: D_p = 0.0013 ft.

ε = 0.352

F_k = 1.117

F_n = 0.4447

Breakthrough Data:

t, sec	C/Co
20.0	0.022
30.0	0.169
40.0	0.387
50.0	0.510
65.0	0.643
75.0	0.705
85.0	0.760
95.0	0.800
115.0	0.836
135.0	0.870
155.0	0.892

Unfavorable Exchange

Column Characteristics: L = 1.657 ft.

D_c = 0.1306 ft.

Solution Characteristics: $\dot{V}$ = 0.77e-03 ft^3/sec

ρ = 62.22 lb/ft^3

μ = 0.0006 lb/ft/sec

C_{in} = 1.979 kb/ft^3

Resin Characteristics: D_p = 0.0012 ft.

ϵ = 0.352
F_k = 1.0985
F_n = 0.38414

Breakthrough Data:

t, sec	C/Co
9.8	0.001
10.1	0.004
10.8	0.020
11.8	0.064
12.8	0.150
13.8	0.227
14.8	0.296
15.8	0.348
16.8	0.395
17.8	0.447
18.8	0.456
19.8	0.488
20.8	0.503
21.8	0.534
22.8	0.543
42.8	0.700
62.8	0.780
82.8	0.833
102.8	0.858

APPENDIX D

TRUNCATION ERROR ANALYSIS

Truncation Error Analysis

The general one-dimensional convection-dispersion equation is given by

$$\varepsilon \frac{\partial C}{\partial t} = D_z \frac{\partial^2 C}{\partial z^2} - V_z \frac{\partial C}{\partial z} . \qquad S_E \qquad (51)$$

The explicit, centered-difference representation of Equation 51 is given by

$$\frac{\varepsilon}{\Delta t} [C(z, t+\Delta t) - C(z,t)] \qquad S_A \qquad (52)$$

$$= \frac{D_z}{(\Delta z)^2} [C(z+\Delta z,t) - 2 C(z,t) + C(z-\Delta z,t)]$$

$$- \frac{V_z}{2\Delta z} [C(z+\Delta z,t) - C(z-\Delta z,t)]$$

Truncation is inherent in the solution of Equation 52. This error is quantified by subtracting the exact equation (Equation 51) from the approximated equation (Equation 52).

$$E_T = S_A - S_E , \qquad (53)$$

where

E_T = truncation error,

S_A = approximated equation,

and

S_E = exact equation.

Expressing the finite-difference terms as Taylor series expansions, and keeping terms up to second order in the increments, gives

$$C(z,t+\Delta t) - C(z,t) = \Delta t \frac{\partial C}{\partial t} + \frac{(\Delta t)^2}{2} \frac{\partial^2 C}{\partial t^2} , \tag{54}$$

and

$$C(z+\Delta z,t) - C(z-\Delta z,t) = 2\Delta z \frac{\partial C}{\partial z} . \tag{55}$$

Substitution of Equations 54 and 55 into Equation 52 gives

$$S_A = \varepsilon \left[\frac{\partial C}{\partial t} + \frac{\Delta t}{2} \frac{\partial^2 C}{\partial t^2} \right] - \{ D_z \frac{\partial^2 C}{\partial z^2} - V_z \frac{\partial C}{\partial z} \} \tag{56}$$

$$S_E = \varepsilon \frac{\partial C}{\partial t} - \{ D_z \frac{\partial^2 C}{\partial z^2} - V_z \frac{\partial C}{\partial z} \} . \tag{57}$$

Subtracting Equation 57 from Equation 56 gives the expression for E_T,

$$E_T = \varepsilon \frac{\Delta t}{2} \frac{\partial^2 C}{\partial t^2} . \tag{58}$$

The error can be converted to a more revealing form by rewriting the $\partial^2 C/\partial t^2$ term.

Equation 51 is the first differentiated with respect to t:

$$\varepsilon \frac{\partial^2 C}{\partial t^2} = D_z \frac{\partial^3 C}{\partial z^2 \partial t} - V_z \frac{\partial^2 C}{\partial z \partial t} \tag{59}$$

Neglect third-order iterated partial derivatives to obtain

$$\varepsilon \frac{\partial^2 C}{\partial t^2} = - V_z \frac{\partial^2 C}{\partial z \partial t} \tag{60}$$

Expressions for the second-order derivatives are obtained by differentiating Equation 51 with respect to z:

$$\varepsilon \frac{\partial^2 C}{\partial z \partial t} = D_z \frac{\partial^3 C}{\partial z^3} - V_z \frac{\partial^2 C}{\partial z^2} \qquad (61)$$

Again, third-order derivatives are neglected to give

$$\varepsilon \frac{\partial^2 C}{\partial z \partial t} = - V_z \frac{\partial^2 C}{\partial z^2} \qquad (62)$$

From Equations 60 and 62,

$$\frac{\partial^2 C}{\partial t^2} = - \frac{V_z}{\varepsilon} \frac{\partial^2 C}{\partial z \partial t} , \qquad (63)$$

and

$$\frac{\partial^2 C}{\partial z \partial t} = - \frac{V_z}{\varepsilon} \frac{\partial^2 C}{\partial z^2} \qquad (64)$$

Then

$$\frac{\partial^2 C}{\partial t^2} = - \frac{V_z}{\varepsilon} \left(- \frac{V_z}{\varepsilon} \frac{\partial^2 C}{\partial z^2} \right) . \qquad (65)$$

Substituting Equation 65 into Equation 58 yields

$$E_T = \frac{\Delta t}{2} \left(\frac{V_z^2}{\varepsilon} \frac{\partial^2 C}{\partial z^2} \right) . \qquad (66)$$

From Equation 53,

$$S_A = S_E + E_T \tag{67}$$

Therefore, from Equations 57 and 58,

$$S_A = \varepsilon \frac{\partial C}{\partial t} - D_z \frac{\partial^2 C}{\partial z^2} + \varepsilon \frac{\Delta t}{2} \frac{\partial^2 C}{\partial t^2} + V_z \frac{\partial C}{\partial z} \,. \tag{68}$$

E_t or from (65)

Now, Equation 65 is inserted to give

$$S_A = \varepsilon \frac{\partial C}{\partial t} - [D_z + \frac{V_z^2}{\varepsilon} \frac{\Delta t}{2}] \frac{\partial^2 C}{\partial z^2} + V_z \frac{\partial C}{\partial z} \,. \tag{69}$$

The solution of $S_A = 0$ is the desired solution. Therefore, Equation 69 is rewritten

$$\varepsilon \frac{\partial C}{\partial t} = [D_z - \frac{V_z^2}{\varepsilon} \frac{\Delta t}{2}] \frac{\partial^2 C}{\partial z^2} - V_z \frac{\partial C}{\partial z} \,. \tag{70}$$

The above truncation error analysis shows that the solution of the difference equation $S_A = 0$ corresponds to Equation 70, not the original Equation 51. The difference is due to E_T, which appears as an alteration of the dispersion coefficient. This alteration is given by

$$D_{ztot} = D_z - D_{znum} \tag{71}$$

where

$$D_{znum} = \frac{1}{2} V_z^2 \frac{\Delta t}{\varepsilon} \,.$$

VITA

Keith Josef Wilson

Candidate for the Degree of

Master of Science

Thesis: SIMULATION OF FIXED-BED ION EXCHANGE PROCESSES

Major Field: Chemical Engineering

Biographical:

Personal Data: Born in Greensboro, North Carolina, October 1, 1960, the son of Josef B. and Dale D. Wilson.

Education: Graduated from McGacock Comprehensive High School, Nashville, Tennessee, in June 1978; received Degree of Bachelor of Science in Chemical Engineering from Tennessee Technological University in August, 1982; completed requirements for the Degree of Master of Science at Oklahoma State University in December, 1983.

Professional Experience: Two summers in production with Aladdin Industries, Inc., Nashville, Tennessee, 1980 and 1981; Teaching Assistant, School of Chemical Engineering, Oklahoma State University, August to December, 1982; Research Assistant, Water Research Center, Oklahoma State University, January to December, 1983.